

Time evolution copulas in FX market



Ledys Llasmin Salazar Gomez

Advisor: Prof. Milan Stehlik

Coadvisor: Prof. Soledad Torres

Instituto de Estadística

Universidad de Valparaíso

This dissertation is submitted for the degree of

Doctora en Estadística

January 2019

Executive Summary

Foreign currencies fluctuate through the international money market. This market sets the different exchange values according to economic variables, such as: VAT, inflation, GDP, and others. Importantly, currency fluctuation significantly influences the economy; and currency trading also affects trade relations between countries.

Thus, endogenous and/or exogenous variables that may be dependent over time affect some currencies' behavior and currencies' interaction with other currencies. Authors such as Escarela and Hernández (2009), Kamal and Haque (2016), Cherubini et al. (2013), among others, have addressed this issue.

In accordance with the proposed objectives, this thesis is divided into five chapters. In the first and second chapters, we present the preliminary concepts of copulas theory and stochastic processes, respectively. In the Chapter 3, we investigate copulas' time evolution, well visible in such a dynamic market as the FX market. We first show how several copula families evolve in time for EUROJPY and CHFJPY in the FX market. The Black-Scholes paradigm suggests applying evolution of copulas with respect to heat equation (see Ishimura (2014)). Stationary limit of such evolution is proven an independent copula under strong regularity conditions. However, empirical observations of FX stock confirm that the real market can be more complicated, because of FX market violations. We show that under slight changes of topology the limiting object is not a copula, because the 1-Lipschitzianity continuity is violated (see Kupka et al. (2018)).

As for the copula functions, they have great potential when capturing the dependence structure between the variables through the monotone and/or counter-monotone properties between them. These two properties are evident in some dependent measures such as Kendall's τ and Spearman's ρ . Therefore, we focus on: a) the extraction of different subsamples, b) the construction of the copula function, and c) the calculation of the Kendall's τ and Spearman's ρ coefficients for each one of them.

Particularly, we observe the divergence of the Kendall's τ coefficient as the number of subsamples increases, i.e., instability in the emerging copula is evident in time evolution. Additionally, the parameters of the copulas do not show specific patterns, i.e., it is not possible to ensure convergence. No less important is that FX market time series present a high volatility and erratic probabilistic behavior. Ishimura and Yoshizawa's (2011) proposed a method to construct bivariate copulas that evolve with the time variable, and determined the convergence of these copulas sequence. In addition, they guaranteed that the convergence in the copulas sequence is explicit in the Product copula, thanks to the accomplishment of some assumptions.

In this sense, Chapter 3 complements Ishimura and Yoshizawa's (2011) study because it offers the possibility of visualizing divergent behavior in a sequence of copulas.

In Chapter 4, we propose the TCLM (t-student copula and long memory) model to understand the subjacent stochastic process in the financial series studied. Initially, we define the returns of each currency, and then the joint behavior through the construction of the 2-dimensional copula. This way, we dedicate part of this study to analyzing the distributional assumption of the data, in this case, the distributional assumption of the returns. For financial returns that exhibit a non-Gaussian behavior, in particular a t-student behavior, Sánchez (2015) offers the possibility of transforming the random t-student variable into a random Gaussian variable.

Finally, we proceed with the analysis of memory. We present $\hat{\nu}$ in the t-student distribution and bivariate Gaussian processes, the H parameter estimation with DWT, the coherence function between the increments of a FMB 2-dimensional, the construction of the TCLM model, the non-Gaussian bivariate processes and data analysis. The initial phase shown in Chapter 4, allowed us to visualize the distribution of returns, which do not always follow a Gaussian distribution. In addition, the 2-dimensional copula illustrated a behavior of extreme value copulas, specifically the t-student.

The multivariate Gaussian distribution has the property that each marginal one is Gaussian. In addition, if the covariances are zero, the random variables are independent. For this work, all covariances are different from zero, i.e., dependence exists between the variables. Then, we proceed with the extraction of univariate Gaussian distributions and analyze their behavior. First, we verify some assumptions: stationary increments, self-similarity and dependence among the increments. Second, we analyze memory. That is, once the Gaussian random variable and the accomplishment of the assumptions are known, we estimate the value of H_1 and H_2 for each of the marginal ones. Shevchenko (2014), Bahamonde (2014) and Villa (1998) treat H as a parameter that quantifies the memory of the process. To estimate H different methods exist: generalized quadratic variation, wavelet coefficients, aggregate variance, rescaled range, discrete wavelet transformation, among others (see Abry et al. (2000), Jones et al. (1996), Kirichenko et al. (2011), Bahamonde (2014)). In this study, we use the DWT for the H estimation. The information of the copula, together with the values of H_1 and H_2 , allow an approximation to the nature of the stochastic process subjacent in the financial series studied. Additionally, we present the coherence function, in a way to enable visualizing the relationship between the two trajectories.

Finally, we present the construction and application of the TCLM model in real and simulated data. For real data, we use the value of the CHFJPY and EUROJPY currencies of the Japanese Bank; and for simulated data, we generate two FBMs.

Our results become key to analyze the dependence between two currencies. As result of analyzing subsamples in Chapter 3, and long memory and the implicit stochastic process in Chapter 4, it becomes clear that both aspects provide useful information for the analysis, construction and prediction of models in finance.

To those who accompanied me during the entire process: David Muñoz and Santiago Muñoz.
My great inspiration.

Acknowledgements

Dr. Milan Stehlik and Dra. Soledad Torres facilitated the academic formation that enabled the development of this research. With their support I could produce the work necessary for my thesis, for which I express my gratitude to both.

I'm also grateful for the university, academics, friends and family who supported me. Special thanks go to Dr. Carlos Henríquez, Dr. Harvey Rosas and Dr. Rodrigo Salas, whose teachings and support were crucial in this process. Also, special thanks go to Yubiceli Salazar.

David Muñoz deserves my sincere gratefulness for his unconditional support. I thank him and Santiago Muñoz for giving me great inspiration and joy.

Abstract

Spanish Version

La estructura de dependencia en el tiempo para las variables que influyen en el mercado de divisas desempeña un papel clave en la toma de decisiones, especialmente cuando se desea movilizar capital. Nuestra investigación se centra en este aspecto; el objetivo principal es analizar la estructura de la dependencia en procesos estocásticos asociados al mercado de divisas a través de la construcción de cópulas bidimensionales que evolucionan con el tiempo. Por lo tanto, abordamos el tema en cinco capítulos. En los Capítulos 1 y 2, ilustramos los conceptos preliminares de la teoría de cópulas y procesos estocásticos. En el Capítulo 3 exponemos el análisis de submuestras construyendo cópulas bidimensionales e ilustramos su evolución temporal en el mercado de divisas. También, analizamos la convergencia de la secuencia de cópulas y mostramos que esta secuencia no converge a la cópula Producto, excepto bajo condiciones regularidad fuerte. Adicionalmente, mostramos que bajo ligeros cambios de topología, el límite no es una cópula porque se viola la propiedad 1-Lipschitz. En el Capítulo 4, proponemos el modelo TCLM como una herramienta útil para analizar un proceso estocástico bivariado no gaussiano. Utilizamos la cópula t-student y los coeficientes de dependencia en colas para analizar la convergencia en los grados de libertad del proceso. Asimismo, determinamos el parámetro H en cada una de las trayectorias usando la DWT y, finalmente, analizamos la función de coherencia entre los incrementos de ambas trayectorias. En el Capítulo 5 presentamos conclusiones, preguntas abiertas y delineamos el potencial para futuros trabajos.

Además, en el Capítulo 3 ilustramos la monotonía y la contramonotonía en las cópulas construídas mediante la evolución del coeficiente τ (*Kendall's tau*) en cada submuestra. Los resultados indican que la secuencia de cópulas no es convergente. Adicionalmente, mostramos la prevalencia de distribuciones de valores extremos en el mercado de divisas. En el Capítulo 4, demostramos la importancia de estimar correctamente el parámetro H para reconocer la naturaleza del proceso estocástico subyacente. También, ilustramos que las series del mercado de divisas presentan con frecuencia comportamientos diferente al

gaussiano. Finalmente, este conjunto de aspectos fue capturado en el modelo propuesto TCLM. Los fundamentos presentados en el Capítulo 3 se aplicaron a datos reales, y los del Capítulo 4 a datos reales y simulados. Para ambos capítulos, los datos reales corresponden al valor de las monedas EUROJPY y CHFJPY de un banco japonés, y los datos simulados a dos trayectorias de un FBM.

English Version

The structure of time dependence for variables that influence the FX market plays a key role in decision-making, especially when the aim is to mobilize capital. Our research focuses on this latter aspect; the main objective is to analyze the structure of dependence in stochastic processes associated with the FX market through the construction of 2-dimensional copulas that evolve over time. We address the topic in five chapters. In Chapter 1 and Chapter 2 we illustrate the preliminary concepts of copula theory and stochastic processes. In Chapter 3 we expose the analysis of subsamples by constructing 2-dimensional copulas and illustrate their temporal evolution in the FX market. Additionally, we analyzed the convergence of the copula sequence and show that this sequence does not converge into the Product copula, except under conditions of strong regularity. In addition, we show that under slight changes of topology, the limit is not a copula, because the 1-Lipschitz property is violated. In Chapter 4, we propose the TCLM model as a useful tool to analyze a non-Gaussian bivariate stochastic process. We used the t-student copula and the dependence coefficients in tails to analyze the convergence in the degrees of freedom of the process. Additionally, we determine the H parameter in each of the trajectories using the DWT, and finally, we analyze the coherence function between the increments of both trajectories. In Chapter 5 we present conclusions, open questions and outline potential for future works.

Moreover, in Chapter 3 we illustrate the monotony and countermonotony in the copulas constructed by the evolution of the Kendall's τ coefficient in each subsample. Results indicate that the sequence of copulas is not convergent. Additionally, we show the prevalence of extreme value distributions in the FX market. In Chapter 4, we further demonstrate the importance of correctly estimating the H parameter for recognizing the nature of the subjacent stochastic process. In addition, we show that the FX market series frequently present behaviors different to gaussian. Finally, this set of aspects was captured in the proposed TCLM model. The fundamentals presented in Chapter 3 were applied to real data, and those in Chapter 4 to real and simulated data. For both chapters, real data correspond to the value of the EUROJPY and CHFJPY currencies of the Japanese Bank, and the simulated data to two trajectories of an FBM.

Table of contents

List of figures	xiii
List of tables	xv
1 Background of copula's theory	5
1.1 Definitions	5
1.2 The Fréchet-Hoeffding bounds	9
1.3 Dependence measures	10
1.4 Graphical dependence measures	12
1.5 Survival Copulas	13
1.6 Archimedian Copulas	14
1.7 Extreme Value Copulas	15
1.8 Copulas with specified properties	17
2 Stochastic Processes	19
2.1 Stochastic processes definition	19
2.2 Brownian motion	20
2.3 Fractional Brownian motion	21
2.4 Hurst parameter estimation	21
2.5 Autocorrelation function	22
2.6 Hurst parameter in Finance	22
3 Time copulas evolution	25
3.1 FX market	26
3.2 Methods of constructing copulas	26
3.3 Time evolutions of copulas and FX markets	28
3.4 1-Lipschitzian	28
3.5 FX illustration of copula evolution	30
3.6 Dependence measures	34

3.7	Copulas observed in FX data	36
3.7.1	t-student Copula	36
3.7.2	Tawn Copula	36
3.7.3	Gumbel Copula	37
3.7.4	Frank Copula	37
3.7.5	Archimedean Copula	37
3.7.6	Family BB8 Copula	37
4	Assessment of long memory in non-Gaussian process using copulas	39
4.1	Degrees of freedom parameter in the t-student distribution and bivariate Gaussian process	39
4.2	Hurst parameter estimation with DWT	40
4.3	Covariance function on the 2-dimensional FBM	41
4.4	Construction of the TCLM model	42
4.5	Non-gaussian bivariate process	44
4.6	Analysis data	45
4.6.1	Real data	45
4.6.2	Simulated data	49
5	Conclusions, open questions and future works	53
5.1	Time copulas evolution	53
5.2	Assessment of long memory estimation in non-Gaussian process using copulas	54
5.3	Open questions and future works	55
	References	57
	Appendix A Chapter I	61
	Appendix B Chapter III	69
	Appendix C Chapter IV	77

List of figures

3.1	Time series of the CHFJPY and the EUROJPY.	25
3.2	Time series of the return CHFJPY.	26
3.3	Time series of the return EUROJPY.	26
3.4	Kendall's τ (50, 100, 500 and 1000 samples).	31
3.5	Graphical illustration of time evolution of parameters in the copulas.	32
3.6	dcopula t-student for the 5 sample.	34
3.7	dcopula t-student for the 548 sample.	34
3.8	Upper and lower bounds for Spearman's ρ coefficient.	35
3.9	Upper and lower bounds for Kendall's τ coefficient.	35
4.1	Method construction of the TCLM model.	43
4.2	Returns of the CHFJPY.	44
4.3	Returns of the EUROJPY.	44
4.4	Density t-student copula.	45
4.5	Level curves t-student copula.	45
4.6	t-student copula for the CHFJPY and EUROJPY returns.	46
4.7	Convergence of degrees of freedom ($\hat{\nu}$) on the t-student copula.	47
4.8	Regression line return CHFJPY.	47
4.9	Regression line return EUROJPY.	47
4.10	Stochastic process reconstructed (real data).	48
4.11	Coherence function (ellipse on real data).	49
4.12	$FBM_1, H_1 = 0.89$	50
4.13	$FBM_2, H_2 = 0.87$	50
4.14	Regression line FBM_1	50
4.15	Regression line FBM_2	50
4.16	Coherence function (ellipse on simulated data).	51

List of tables

3.1	Total data for 50, 100, 500 and 1000 groups.	31
3.2	Evolution of parameters of copulas for the first 10 groups.	32
3.3	Frequency of the copulas in the samples.	33
4.1	\hat{H}_1 and \hat{H}_2 using DWT (real data).	48
4.2	Regression lines of the FBM_1 and FBM_2 (simulated data).	50

Introduction

The FX market continuously illustrates greatly versatile financial time series. Especially, time series that contain currency returns are distinguished by their wide volatility and instability. This is the main driver behind the development of this thesis.

An essential aspect when studying FX market time series, specifically, those with the value of some currency, relates to the behavior of returns. For example, Markowitz in the theory of portfolio construction established that returns are Gaussian distributed. Yet, in real data sets this assumption is not always valid. Hence, it is essential to analyze the distribution assumption for the construction of portfolios or the elaboration of forecasting models.

In addition, we must be careful in the analysis of probabilistic behavior of the data, in some cases the focus of study may be on marginal and joint distributions behavior. In this sense, we analyze the dependence structure in stochastic processes associated with the FX market through the construction of 2-dimensional copulas.

Copula functions are mathematical functions that accomplish the boundary conditions and are characterized by be increases (see Nelsen (2006)). As Escarela and Hernández (2009) state: "The use of copulas is attractive because it allows a great flexibility to model the joint distribution of a random pair that can arise from practically any discipline, and it does so simply because they only need to specify the copula function and the marginal ones ". With these notions, we developed this thesis in five chapters. In Chapter 1 and Chapter 2 we present preliminary concepts of the theory of copulas and stochastic processes. In Chapter 3, we present the evolution of copulas in time by extracting subsamples from time series. The series of interest corresponds to the value of the CHFJPY and EUROJPY currencies of the Japanese Bank. Each time series represents an embodiment of the bivariate process, and for this reason, we proceed with the construction of the 2-dimensional copula for each subsample. This way the joint behavior of both series is captured. Once the copula sequence is constructed, we analyze the behavior of its parameters and the value of the Kendall's τ coefficient.

In the process, we find that the sequence of copulas is not convergent; however, it converges to a Product copula under strong regularity conditions (see Ishimura (2014)). In addition, we show that under slight changes of topology, the limit is not a copula because the 1-Lipschitz property is violated (see Kupka et al. (2018)).

In Chapter 4, we propose the TCLM model for the analysis of non-Gaussian bivariate stochastic processes. To define the model, we start with the analysis of the 2-dimensional copula of the whole data set, where we find the behavior of a copula of extreme values, in this case, the t-student. For this reason, we proceed with the transformation of the random t-student variable to a bivariate Gaussian. This allows to obtain the univariate Gaussians, which then serve to estimate the Hurst parameters, H_1 and H_2 respectively. The advantage of estimating H_1 and H_2 , together with the construction of the copula associated with the two time series, allows us to describe the bivariate stochastic process.

We emphasize with the obtained results carry import for the accomplishment of the assumptions at the time of analyzing the BM or FBM, and the link that may exist between the bivariate t-student and bivariate Gaussian distributions. Consequently, the ideas presented throughout this thesis provide theoretical and practical foundations for the analysis of financial series. Another important aspect in this thesis is the analysis of the memory of the process. Although each time series represents a trajectory of the same, the joint behavior can be visualized with close values between H_1 and H_2 .

We argue that this thesis is a useful tool for the analysis of the stochastic process associated with financial time series of the FX market. Additionally, the proposed methodology allows us to join the foundations of the Theory of Copulas and Stochastic Processes, within the framework of dependence associated with the variables of the process, to the respective non-Gaussian behavior.

Further work is needed to investigate stochastic processes involving the behavior of three or more currencies. Additionally, the possibility of using the results obtained in the construction of portfolios and the evaluation of long memory models remains a problem.

Abbreviations and Symbols

Abbreviations

AR: Autoregressive.

ARFIMA: Autoregressive fractionally integrated moving average.

ARMA: Autoregressive moving average.

BM: Brownian motion.

CDF: Cumulative distribution function.

CHF: Swiss franc.

CHFJPY: Swiss franc - Japanese yen.

DWT: Discrete Wavelet Transformation.

EUR: Euro.

EUROJPY: Euro - Japanese yen.

FBM: Fractional Brownian motion.

FOREX or FX: Foreign Exchange.

GBP: Pound Sterling.

GDP: Gross inner product.

H: Hurst parameter or the Hurst index.

JPY: Japanese yen.

MA: Moving average.

ML: Maximum Likelihood.

TCLM: t-copula and long memory model.

VAT: Value added tax.

Symbols

I: Unit interval.

$\Pi(u, v)$: Product copula (Harmonic copula).

$d_{j,k}$: Detail coefficients in the DWT.

$a_{j,k}$: Scale coefficients in the DWT.

\neg : Negation.

$\overline{\mathbb{R}}$: Real extended.

φ : Continuous and non-increasing function on $[0, \infty]$.

$\varphi^{[-1]}$: Pseudo-inverse of φ .

τ : Kendall's *tau* coefficient.

ρ : Spearman's *rho* coefficient.

λ : Tail dependence coefficient.

Chapter 1

Background of copula's theory

Recent models based on copula functions have been applied in several scientific areas, such as: Finance, Biomedical Sciences, Industrial Processes, Geostatistics, Marine Biology, among others (see Wei and Kim (2018), Liu et al. (2016), Quintero et al. (2017), Allamehzadeh et al. (2015) and Zhang et al. (2011)). Its potential lies in the possibility of modeling situations that include a dependence structure among random variables. In this regard, Sklar (1959) presents an interesting result in his famous theorem (Sklar's Theorem). Sklar states that if there is a joint distribution function with their respective marginal distribution functions, then there is a copula; and that it is possible to write the function of joint distribution in terms of the copula and the inverse of the marginals.

Specifically, in the financial area, there is a high interest in establishing the relationship between the joint distribution function and their respective marginal distribution functions when the random variables preserve a dependence structure. Particularly, for the FX market it is useful to recognize the behavior of a currency related to one or several currencies. In this particular research we will focus on analyzing the joint behavior between two currencies.

In the Chapter 1 we will present an approach to the definition of the copula function and some definitions.

1.1 Definitions

Definition 1. *Let X and Y be random variables defined on the equal probability space $(\Omega, \mathcal{F}, \mathbb{P})$. The joint bivariate probability distribution function of these random variables is a function $H_{XY} : \mathbb{R}^2 \rightarrow [0; 1]$ defined as (see Erdely (2017))*

$$H_{XY} := H(x, y) := \mathbb{P}(X^{-1}(] - \infty, x]) \cap Y^{-1}(] - \infty, y])). \quad (1.1)$$

As $X^{-1}([-\infty, x]) = \{\omega \in \Omega : X(\omega) \leq x\} \in \mathcal{F}$ and also $Y^{-1}([-\infty, y]) = \{\omega \in \Omega : Y(\omega) \leq y\} \in \mathcal{F}$, it is more common to use simplified notation

$$H(x, y) := \mathbb{P}(X \leq x, Y \leq y). \quad (1.2)$$

Theorem 1. *If $H(x, y)$ is the joint distribution function for the bivariate case, with random variables X and Y , which have probability distribution functions $F(x)$ and $G(y)$, respectively, then (see Erdely (2017)):*

- a. $H(x, -\infty) = 0 = H(-\infty, y)$.
- b. $H(x, +\infty) = F(x)$, $H(+\infty, y) = G(y)$.
- c. $H(+\infty, +\infty) = 1$.
- d. $H(x, y)$ is 2-increasing, i.e. if $x_1 < x_2$, $y_1 < y_2$, then:

$$H(x_2, y_2) - H(x_2, y_1) - H(x_1, y_2) + H(x_1, y_1) \geq 0.$$
- e. $H(x, y)$ is monotone increasing in each variable.
- f. $H(x, y)$ is continuous by the right in each variable.

In the bivariate case, the recognition of marginal distribution functions, together with the construction of function C , called the copula function, represents the essential ingredient for the use of Sklar's theorem.

Theorem 2. *(Sklar theorem) Let $H(x, y)$ be a joint distribution function with margins $F(x)$ and $G(y)$. Then there exists a copula C such that for all x, y in $\overline{\mathbb{R}}$,*

$$H(x, y) = C(F(x), G(y)). \quad (1.3)$$

If $F(x)$ and $G(y)$ are continuous, then C is unique; otherwise, C is uniquely determined on $\text{Ran}F \times \text{Ran}G$. Conversely, if C is a copula and $F(x)$ and $G(y)$ are distribution functions, then the function $H(x, y)$ is a joint distribution function with marginals $F(x)$ and $G(y)$.

From a practical point of view the FX market has as main objective to facilitate the monetary flow. However, companies or financial firms operate to minimize risk and maximize profitability. For this reason, knowing the function of joint distribution that modeled the dependence between two currencies provides probabilistic information that can be used in the analysis of information and decision-making.

In this meaning, we focus on the bivariate distribution function and analyze the stochastic process from their trajectories. However, the key point lies in the construction of the 2-dimensional copula that fulfills each of the assumptions is mentioned in the next definition.

Definition 2. *2-dimensional copula is a function C from \mathbf{I}^2 to \mathbf{I} with the following properties (see Nelsen (2006)):*

1. For every u, v in \mathbf{I} ,

$$C(u, 0) = 0 = C(0, v) \text{ and } C(u, 1) = u \text{ and } C(1, v) = v. \quad (1.4)$$

2. For every u_1, u_2, v_1, v_2 in \mathbf{I} , such that $u_1 \leq u_2$ and $v_1 \leq v_2$,

$$C(u_2, v_2) - C(v_2, v_1) - C(u_1, v_2) + C(u_1, v_1) \geq 0. \quad (1.5)$$

Definition 3. *n -dimensional copula is a function C from \mathbf{I}^n to \mathbf{I} with the following properties (see Cintas (2006)):*

1. For every $\mathbf{u} = (u_1, \dots, u_n)$ in \mathbf{I}^n ,

$$C(\mathbf{u}) = 0 \quad (1.6)$$

if exists some i which $u_i = 0, i = 1, \dots, n$.

And if $\mathbf{u} = (1, \dots, 1, u_k, 1, \dots, 1)$, where $u_k < 1$ for some k , then,

$$C(\mathbf{u}) = u_k. \quad (1.7)$$

2. For every \mathbf{a} and \mathbf{b} in \mathbf{I}^n , such that $\mathbf{a} \leq \mathbf{b}$,

$$V_C([\mathbf{a}, \mathbf{b}]) \geq 0. \quad (1.8)$$

In the present investigation we focus only on the construction of 2-dimensional copula exposed in the Definition 2. Also, it is important to emphasize that to build the bivariate distribution function it is necessary to guarantee the existence of the inverse functions for $F(x)$ and $G(y)$, $F(x)^{-1}$ and $G(y)^{-1}$, respectively.

If a real function is bijective, it has an associated inverse function. However, it is not always possible to ensure the accomplishment of this property. Specifically, when we refer to the cumulative distribution function $F(x)$; we will denote its inverse by $F^{(-1)}$ and we will call this *quasi-inverse*.

Definition 4. Let $F(x)$ be a distribution function. Then a quasi-inverse of F is any function $F^{(-1)}$ with domain \mathbf{I} , such that (Nelsen (2006)),

1. If $t \in \text{Ran}F$, then $F^{(-1)}(t)$ is any number x in $\overline{\mathbb{R}}$ such that $F(x) = t$, i.e., for all t in $\text{Ran}F$,

$$F(F^{(-1)}(t)) = t. \quad (1.9)$$

2. If t is not in $\text{Ran}F$, then,

$$F^{(-1)}(t) = \inf\{x|F(x) \geq t\} = \sup\{x|F(x) \leq t\}. \quad (1.10)$$

If $F(x)$ is strictly increasing, then it has a single quasi-inverse, which is clearly the ordinary inverse, for which we use the customary notation F^{-1} .

Theorem 3. Let $H(x,y)$ the bivariate joint distribution function of X and Y , $F(x)$ the distribution function marginal of X , $G(y)$ distribution function marginal of Y , and $F^{(-1)}$ and $G^{(-1)}$ quasi-inverses of F and G , respectively. Then for any (u,v) in $\text{Dom}C$ (see Nelsen (2006)),

$$C(u,v) = H(F^{(-1)}(u), G^{(-1)}(v)). \quad (1.11)$$

Definition 5. According to Cintas (2006), (for continuous random vectors), the density of the copula is related to the density $h(x,y)$ associated with the joint distribution function $H(x,y)$. Specifically, it is equal to the ratio between the joint density and the product of the marginal densities,

$$c(u,v) = \frac{h(F^{(-1)}(u), G^{(-1)}(v))}{f(F^{-1}(u))g(G^{-1}(v))}. \quad (1.12)$$

Theorem 4. Let S_1 and S_2 be nonempty subsets of $\overline{\mathbb{R}}$, and let $H(x,y)$ be a grounded 2-increasing function with domain $S_1 \times S_2$. Let (x_1, y_1) and (x_2, y_2) be any points in $S_1 \times S_2$. Then

$$|H(x_2, y_2) - H(x_1, y_1)| \leq |F(x_2) - F(x_1)| + |G(y_2) - G(y_1)|. \quad (1.13)$$

The following theorem, which follows directly from previous theorem, establishes the continuity of copulas via a Lipschitz condition on \mathbf{I}^2 (see Nelsen (2006)).

Theorem 5. Let C be a copula, then for every $(u_1, u_2), (v_1, v_2)$ in $\text{Dom}C$,

$$|C(u_2, v_2) - C(u_1, v_1)| \leq |u_2 - u_1| + |v_2 - v_1|, \quad (1.14)$$

hence C is uniformly continuous on $DomC$.

The 1-Lipschitz condition ensure that the copula function is continuous throughout its domain, a fundamental requirement to ensure the existence of the first derivative. Therefore it ensure the existence of the density of the copula.

Another fundamental point in the framework of copula functions has to do with their convergence. The Fréchet-Hoeffding bounds allow us to visualize the oscillation dimensions as shown in the next section (see Nelsen (2006)).

1.2 The Fréchet-Hoeffding bounds

Definition 6. *Fréchet-Hoeffding bounds inequality: Let $M(u, v) = \min(u, v)$ and $W(u, v) = \max(u + v - 1, 0)$. Thus for every copula C and every (u, v) in \mathbf{I}^2 ,*

$$W(u, v) \leq C(u, v) \leq M(u, v). \quad (1.15)$$

In Definition 6, M is the Fréchet-Hoeffding upper bound and W is the Fréchet-Hoeffding lower bound (see Cintas (2006)). For the case of 2-dimensional copula, by the upper and lower bound are copula functions. However, for $n > 2$ the lower bound is not a copula. If any of the Fréchet-Hoeffding bounds corresponds to the Product copula $\Pi(u, v) = uv$, we refered to the copula that characterizes the independence of random variables.

Theorem 6. *Let X and Y be continuous random variables and $\Pi(u, v)$ the Product copula. Then X and Y are independent if and only if*

$$C_{XY} = \Pi(u, v) = uv. \quad (1.16)$$

Remember that in the FX market can be presented in two scenarios: dependence or independence between random variables. In the case of dependence, we must be carefull and analyze its structure, which may be reflected in some measures. For example, comonotonicity and countermonotonicity properties indicate the dependence between the two random variables, as is explained in the next definition.

Definition 7. *In the 2-dimensional case, the fact that the joint distribution of the two random variables is characterized by the upper bound of Fréchet-Hoeffding, M^2 , indicates a situation*

of full positive dependence, also known as comonotonicity. On the contrary, if the copula that binds them is the lower bound of Frechet-Hoeffding, W^2 , also known countermonotonic, indicates a situation of full negative dependence.

The comonotonicity and countermonotonicity can be distinguished in the values, such as: Kendall's τ , Spearman's ρ , Schweizer and Wolff's, and Gini's coefficients. However, in this study we focus on the values of Kendall's τ and Spearman's ρ .

1.3 Dependence measures

According to Nelsen (2006), the concordance and discordance, Kendall's τ and Spearman's ρ coefficients, respectively; are given in the next definitions.

Definition 8. Let (x_i, y_i) and (x_j, y_j) denote two observations from a vector of continuous random variables, (X, Y) . We say that (x_i, y_i) and (x_j, y_j) are concordant if $x_i < x_j$ and $y_i < y_j$, or if $x_i > x_j$ and $y_i > y_j$. Similarly, we say that (x_i, y_i) and (x_j, y_j) are discordant if $x_i < x_j$ and $y_i > y_j$ or if $x_i > x_j$ and $y_i < y_j$.

Definition 9. The Kendall's τ value is the probability of concordance minus the probability of discordance for a pair of observations (x_i, y_i) and (x_j, y_j) that is chosen randomly from the sample and is given by

$$\tau = \tau_{X,Y} = P[(X_1 - X_2)(Y_1 - Y_2) > 0] - P[(X_1 - X_2)(Y_1 - Y_2) < 0]. \quad (1.17)$$

Theorem 7. Let (X_1, Y_1) and (X_2, Y_2) be independent vectors of continuous random variables with joint distribution functions H_1 and H_2 , respectively, with common margins F (of X_1 and X_2) and G (of Y_1 and Y_2). Let C_1 and C_2 denote the copulas of (X_1, Y_1) and (X_2, Y_2) , respectively, so that $H_1(x, y) = C_1(F(x), G(y))$ and $H_2(x, y) = C_2(F(x), G(y))$. Let Q denotes the difference between the probabilities of concordance and discordance of (X_1, Y_1) and (X_2, Y_2) , i.e.,

$$Q = P[(X_1 - X_2)(Y_1 - Y_2) > 0] - P[(X_1 - X_2)(Y_1 - Y_2) < 0]. \quad (1.18)$$

Then,

$$Q = Q(C_1, C_2) = 4 \int \int_{\mathbf{I}^2} C_2(u, v) dC_1(u, v) - 1. \quad (1.19)$$

Theorem 8. Let X and Y be continuous random variables whose copula is C . Then the version of Kendall's τ value for X and Y (which we will denote by either $\tau_{X,Y}$ or τ_C) is

given by

$$\tau_{X,Y} = \tau_C = Q(C,C) = 4 \int \int_{\mathbf{I}^2} C(u,v) dC(u,v) - 1. \quad (1.20)$$

Definition 10. Let (X_1, Y_1) , (X_2, Y_2) and (X_3, Y_3) be three independent random vectors with a common joint distribution function H (whose margins are again F and G) and copula C . The version $\rho_{X,Y}$ of Spearman's rho is defined to be proportional to the probability of concordance minus the probability of discordance for the two vectors (X_1, Y_1) and (X_2, Y_3) , i.e., a pair of vectors with the same margins, but one vector with distribution function H , while the components of the other are independent. The Spearman's rho value is given by

$$\rho_{X,Y} = 3 (P[(X_1 - X_2)(Y_1 - Y_3) > 0] - P[(X_1 - X_2)(Y_1 - Y_3) < 0]). \quad (1.21)$$

The joint distribution function of (X_1, Y_1) is $H(x, y)$ and the joint distribution function of (X_2, Y_3) is $F(x)G(y)$, because X_2 and Y_3 are independent. Thus the copula of X_2 and Y_3 is Π .

Theorem 9. Let X and Y be two continuous random variables whose copula is C . Then the version of Spearman's rho value for X and Y (which we will denote by either $\rho_{X,Y}$ or ρ_c) is given by

$$\rho_{X,Y} = \rho_c = 3Q(C, \Pi) = 12 \int \int_{\mathbf{I}^2} uv dC(u,v) - 3 = 12 \int \int_{\mathbf{I}^2} C(u,v) dudv - 3. \quad (1.22)$$

Additionally, the expression 1.22 is equal to

$$\rho_{X,Y} = 12 \int \int_{\mathbf{I}^2} C(u,v) dudv - 3 = 12 \int \int_{\mathbf{I}^2} [C(u,v) - uv] dudv. \quad (1.23)$$

Theorem 10. Let X and Y be continuous random variables, and let τ and ρ denote Kendall's tau and Spearman's rho, previously defined. Then

$$-1 \leq 3\tau - 2\rho \leq 1. \quad (1.24)$$

The mentioned dependence measures, also known as concordance's measures, determine the non-linear relationships between the variables, which is not possible with the linear correlation coefficient. For the bivariate case, when the value of Kendall's tau and Spearman's

ρ reach 1, the corresponding copula is the upper bound of Fréchet-Hoeffding (comonotonicity); and when both coefficients reach -1 , it is the lower bound of Fréchet-Hoeffding (countermonotonicity).

Other measures of dependence are the coefficients of dependence on tails; which reflect the behavior of some extreme value copula. In this thesis, we aim to analyze the behavior of extremes value copulas, which will be specified forward. The extreme values copulas allow to analyze what happens in the extremes with respect to the expected value of the probability function.

Definition 11. (see Nelsen (2006)) *The upper tail dependence parameter λ_U is the limit (if it exists) of the conditional probability that Y is greater than the $100t$ -th percentile of G given that X is greater than the $100t$ -th percentile of F as t approaches 1, i.e.,*

$$\lambda_U = \lim_{t \rightarrow 1^-} P \left[Y > G^{(-1)}(t) | X > F^{(-1)}(t) \right]. \quad (1.25)$$

Definition 12. (see Nelsen (2006)) *The lower tail dependence parameter λ_L is the limit (if it exists) of the conditional probability that Y is less than or equal to the $100t$ -th percentile of G given that X is less than or equal to the $100t$ -th percentile of F as t approaches 0, i.e.,*

$$\lambda_L = \lim_{t \rightarrow 0^+} P \left[Y \leq G^{(-1)}(t) | X \leq F^{(-1)}(t) \right]. \quad (1.26)$$

It is useful to visualize the dependence on tails in the FX market, since this is modified by the dependence between the variables in the presence of extreme events. For example, an unexpected variation in the value of a currency leads to a transformation in the probability and risk of a foreign currency investment portfolio. In other words, the nature of the stochastic process that describes each of the realizations, that is, each of the time series, is characterized by a process of extreme events.

1.4 Graphical dependence measures

The plot of a copula $z = C(u, v)$, is a continuous surface in the unit cube \mathbf{I}^3 , bounded by the cube of vertices: $(0, 0, 0)$, $(0, 1, 0)$, $(0, 0, 1)$, $(0, 1, 1)$, $(1, 1, 0)$, $(1, 1, 1)$, $(1, 0, 1)$ and $(1, 0, 0)$.

For any copula C it is verified that $W(u, v) \leq C(u, v) \leq M(u, v)$, so that the plot of C remains between the plots of the Fréchet- Hoeffding bounds, that is, the surfaces $z = W(u, v)$ and $z = M(u, v)$. A simple way to presents and compares the graph of a copula, is through its contour diagram (see Cintas (2006)).

Definition 13. *The contour diagram is the graphic representation of the contour lines. The contour lines are sets in \mathbf{I}^n given by $C(u, v) = k$, for a constant k .*

The points $(k, 1)$ and $(1, k)$ belong to the level curve corresponding to the constant k . It is also verified that for any copula C and a given $k \in \mathbf{I}$, the graph of the contour $\{(u, v) \in \mathbf{I}^2 : C(u, v) = k\}$ must remain within the triangle determined by $W(u, v) = k$ and $M(u, v) = k$.

In the Chapter 3 we will illustrate contour diagrams for any copula constructed. Now, we explained some copula families.

1.5 Survival Copulas

From a parametrical approach we can build different families of copulas, but our interest is illustrate the survival, archimedean and the extreme values copulas.

The survival analysis based on the distribution of time until the occurrence of an event, commonly called failure time. However, the survival function is not the survival copula. For this reason, the following section focuses on specifying each of these concepts.

Definition 14. *For a pair (X, Y) of random variables with joint distribution function $H(x, y)$, the joint survival function is given by*

$$\bar{H}(x, y) = P(X > x, Y > y). \quad (1.27)$$

The margins of $\bar{H}(x, y)$ are the functions $\bar{H}(x, -\infty)$ and $\bar{H}(-\infty, y)$, which are the univariate survival functions \bar{F} and \bar{G} , respectively (see Nelsen (2006)).

Definition 15. *2-dimensional survival copula is a function \hat{C} from \mathbf{I}^2 into \mathbf{I} given by*

$$\hat{C}(u, v) = u + v - 1 + C(1 - u, 1 - v). \quad (1.28)$$

Take into account that the survival copula \hat{C} is not the joint survival function \bar{C} for two uniform $(0, 1)$ random variables, whose joint distribution function is the copula C (see Nelsen (2006)) given by

$$\bar{C}(u, v) = P[U > u, V > v] = 1 - u - v + C(u, v) = \hat{C}(1 - u, 1 - v). \quad (1.29)$$

Theorem 11. *If the function \hat{C} from \mathbf{I}^2 into \mathbf{I} is defined by $\hat{C}(u, v) = u + v - 1 + C(1 - u, 1 - v)$, we have*

$$\bar{H}(x, y) = \hat{C}(\bar{F}(x), \bar{G}(y)). \quad (1.30)$$

1.6 Archimedean Copulas

Since X and Y are independent, $H(x, y) = F(x)G(y)$ for all x, y in $\overline{\mathbb{R}}$. The Archimedean copulas are applied only to models with relatively weak dependence or almost null dependence.

Definition 16. Let φ be a continuous, strictly decreasing function from \mathbf{I} to $[0, \infty]$, such that $\varphi(1) = 0$. The pseudo-inverse of φ is the function $\varphi^{[-1]}$ with $\text{Dom}\varphi^{[-1]} = [0, \infty]$ and $\text{Ran}\varphi^{[-1]} = \mathbf{I}$ given by

$$\varphi^{[-1]}(t) = \begin{cases} \varphi^{(-1)}(t), & 0 \leq t \leq \varphi^{[-1]}(0) \\ 0, & \varphi^{[-1]}(0) \leq t \leq \infty. \end{cases} \quad (1.31)$$

$\varphi^{[-1]}(t)$ is continuous and nonincreasing on $[0, \infty]$, and strictly decreasing on $[0, \varphi(0)]$ (see Nelsen (2006)). Furthermore, $\varphi^{[-1]}(\varphi(u)) = u$ on \mathbf{I} , and

$$\varphi(\varphi^{[-1]}(t)) = \begin{cases} t, & 0 \leq t \leq \varphi(0) \\ \varphi(0), & \varphi(0) \leq t \leq \infty \end{cases} = \min(t, \varphi(0)) \quad (1.32)$$

Finally, if $\varphi(0) = \infty$, then $\varphi^{[-1]} = \varphi^{-1}$.

Theorem 12. Let φ be a continuous, strictly decreasing function from \mathbf{I} to $[0, \infty]$, such that $\varphi(1) = 0$, and let $\varphi^{[-1]}$ be the pseudo-inverse of φ defined by (1.31). The function C from \mathbf{I}^2 to \mathbf{I} given by

$$C(u, v) = \varphi^{[-1]}(\varphi(u) + \varphi(v)). \quad (1.33)$$

Then C satisfies the boundary conditions and is 2-increasing for 2-dimensional copula (see Nelsen (2006)).

Theorem 13. Let φ be a continuous, strictly decreasing function from \mathbf{I} to $[0, \infty]$, such that $\varphi(1) = 0$, and let $\varphi^{[-1]}$ be the pseudo-inverse of φ . Then the function C from \mathbf{I}^2 to \mathbf{I} is a copula if and only if φ is convex (see Nelsen (2006)).

Definition 17. Copulas of the form (1.33) are called Archimedean copulas.

The function φ is called a generator of the copula. If $\varphi(0) = \infty$, we say that φ is a strict generator. In this case, $\varphi^{[-1]} = \varphi^{-1}$ and $C(u, v) = \varphi^{-1}(\varphi(u) + \varphi(v))$ is said to be a strict Archimedean copula (see Nelsen (2006)).

Theorem 14. *Let C be an Archimedean copula with generator φ . Then:*

1. *C is symmetric; i.e., $C(u,v) = C(v,u)$ for all u,v in \mathbf{I} .*
2. *C is associative, i.e., $C(C(u,v),w) = C(u,C(v,w))$ for all u,v,w in \mathbf{I} .*
3. *If $c > 0$ is any constant, then $c\varphi$ is also a generator of C .*

The Archimedean copulas are in the group of parametric copulas. However, it is important to remember that there are nonparametric copulas where their empirical structure fits the data. Between the parametric copulas can be mentioned: the Gaussian, the t -student, the elliptical, the Archimedean (Frank, Gumbel, Glayton), the HRT (Survival copula of the clayton family), the extreme values, among others.

Now, we will studied the extreme values copula in the next definition, that frequently used in financial area.

1.7 Extreme Value Copulas

According to Genest et al. (2011), the families of left tail decreasing are classified into three groups; Symmetric extreme-value copulas: Gumbel-Hougaard (GH), Galambos (GA), Husler-Reiss (HR) and Student extreme value (t-EV) with four degrees of freedom; Symmetric non-extreme-value copulas: Clayton (C), Frank (F), Normal (N) and Plackett (P); Asymmetric extreme-value copulas: Asymmetric Gumbel–Hougaard (a-GH), Asymmetric Galambos (a-GA), Asymmetric Husler–Reiss (a-HR); and Asymmetric Student extreme-value and copula with four degrees of freedom (a-t-EV).

Theorem 15. *If C is a copula and n a positive integer, then the function $C_{(n)}$ given by*

$$C_{(n)}(u,v) = C^n(u^{\frac{1}{n}}, v^{\frac{1}{n}}), \quad (1.34)$$

for u,v in \mathbf{I} , is a copula. Furthermore, if (X_i, Y_i) , $i = 1, 2, \dots, n$, are independent and identically distributed pairs of random variables with copula C , then $C_{(n)}$ is the copula of $X_{(n)} = \max\{X_i\}$ and $Y_{(n)} = \max\{Y_i\}$ (see Nelsen (2006)).

The limit of the sequence $\{C_{(n)}\}$ from Theorem (1.34) leads to the notion of an extreme value copula.

Definition 18. *A copula C_* is an extreme value copula if there exists a copula C such that*

$$C_*(u,v) = \lim_{n \rightarrow \infty} C^n(u^{\frac{1}{n}}, v^{\frac{1}{n}}), \quad (1.35)$$

for u, v in \mathbf{I} . Furthermore, C is said to belong to the domain of attraction of C_* (see Nelsen (2006)).

Definition 19. A copula C is max-stable if for every positive real number r and all u, v in \mathbf{I} (see Nelsen (2006)), we have that

$$C(u, v) = C^r(u^{\frac{1}{r}}, v^{\frac{1}{r}}). \quad (1.36)$$

Theorem 16. A copula is max-stable if and only if it is an extreme value copula (see Nelsen (2006)).

Let C be a max-stable copula, and let X and Y the two standard exponential random variables whose survival copula is C . Thus the survival functions of X and Y are $\bar{F}(x) = e^{-x}$, $x > 0$, and $\bar{G}(y) = e^{-y}$, $y > 0$, respectively, and the joint survival function is given by

$$\bar{H}(x, y) = P(X > x, Y > y) = C(e^{-x}, e^{-y}). \quad (1.37)$$

Because C is max-stable,

$$\bar{H}(rx, ry) = C^r(e^{-x}, e^{-y}) = [\bar{H}(x, y)]^r \quad (1.38)$$

for any real $r > 0$. Define a function $A : [0, 1] \rightarrow [\frac{1}{2}, 1]$ by

$$A(t) = -\ln C(e^{-(1-t)}, e^{-t}), \quad (1.39)$$

or equivalently, $C(e^{-(1-t)}, e^{-t}) = \exp(-A(t))$. Employing the change of variables $(x, y) = (r(1-t), rt)$ for $r > 0$, and t in $(0, 1)$ [or equivalently, $(r, t) = (x+y, y/(x+y))$], we have

$$\begin{aligned} \bar{H}(x, y) &= \bar{H}(r(1-t), rt) \\ &= [\bar{H}((1-t), t)]^r \\ &= C^r(e^{-(1-t)}, e^{-t}) \\ &= \exp(-rA(t)) \\ &= \exp\left\{-(x+y)A\left(\frac{y}{x+y}\right)\right\}. \end{aligned} \quad (1.40)$$

Because $C(u, v) = H(-\ln u, -\ln v)$, we have proven that C is an extreme value copula (see Nelsen (2006)).

Definition 20. A copula C is an extreme value copula if there exists a copula C such that

$$C(u, v) = \exp \left\{ \ln (uv) A \left(\frac{\ln v}{\ln (uv)} \right) \right\}, \quad (1.41)$$

for u, v in \mathbf{I} .

The function A is called the dependence function of the extreme value copula C . For the right side of (1.41) to define a copula requires that $A : [0, 1] \rightarrow [\frac{1}{2}, 1]$ must satisfy the following conditions: $A(0) = A(1) = 1$, $\max\{t, 1-t\} \leq A(t) \leq 1$, with A a convex function.

In this reseach we will study as copula of extreme values the t-student copula.

1.8 Copulas with specified properties

Definition 21. Let C be a copula with continuous second-order partial derivatives on $(0, 1)^2$. Then C is Harmonic in \mathbf{I}^2 if C satisfies Laplace's equation in $(0, 1)^2$ (see Nelsen (2006)),

$$\nabla^2 C(u, v) = \frac{\partial^2}{\partial u^2} C(u, v) + \frac{\partial^2}{\partial v^2} C(u, v) = 0. \quad (1.42)$$

Definition 22. A copula C is convex if for all (a, b) and (c, d) in \mathbf{I}^2 and λ in \mathbf{I} (see Nelsen (2006)),

$$C(\lambda a + (1 - \lambda)c, \lambda b + (1 - \lambda)d) \leq \lambda C(a, b) + (1 - \lambda)C(c, d). \quad (1.43)$$

Chapter 2

Stochastic Processes

A time series represents the realization of the stochastic process, that is, it is possible to recognize or not some characteristics of the process by analyzing in detail some of its trajectories. The theory of stochastic processes is applicable in different areas of knowledge, e.g.: Physics, Biology, Chemistry, Finance, among others. Typically, in the financial area the time series are highly volatile and some assumptions are not accomplished at the time of applying any concept or model.

In this chapter some basic definitions of stochastic processes are presented, which will allow us to deal in a better form with the ideas presented in the next chapters.

2.1 Stochastic processes definition

Definition 23. According to Mikosch (1999), a stochastic process X is a collection of random variables $X_t, t \in T = X_t(\omega), t \in T, \omega \in \Omega$, defined on some space Ω . A stochastic process X is a function of two variables that:

- For a fixed instant of time t , it is a random variable: $X_t = X_t(\omega), \omega \in \Omega$.
- For a fixed random outcome $\omega \in \Omega$, it is a function of time: $X_t = X_t(\omega), t \in T$.

There are different classes of Stochastic Processes, however, the BM and the FBM are used with great frequency in different areas, particularly in the FX market.

2.2 Brownian motion

Definition 24. According to Mikosch (1999), a stochastic process $B = (B_t, t \in [0, \infty))$ is called (standard) Brownian motion or a Wiener process if the following conditions are satisfied:

- It starts at zero, $B_0 = 0$.
- It has stationary and independent increments.
- For every $t > 0$, B_t has a Gaussian distribution, $N(0, t)$.
- It has a continuous sample paths (no jumps).

A stationary Gaussian processes $X = X_t(w)$, $t \in T$ with $t \in [0, \infty)$ or $T = \mathbb{Z}$, is determined by its expectation and covariance function: $\mu_X(t+h) = \mu_X(t)$ and $c_X(t, s) = c_X(t+h, s+h)$, for all $s, t \in T$, such that $s+h, t+h \in T$. But this means that $\mu_X(t) = \mu_X(0)$ for all t , whereas $c_X(t, s) = \tilde{c}_X(|t-s|)$ for some function \tilde{c} . Hence, for a Gaussian process, strictly stationary means that the expectation function is constant and the covariance function only depends on the distance $|t-s|$. More generally, if a (possibly non-Gaussian) process X has the two aforementioned properties, it is called a stationary (in the wide sense) or (second order) stationary process (see Mikosch (1999)).

Stationary can also be imposed on the increments of a process. The process itself is then not necessarily stationary.

Definition 25. Let $X = (X_t, t \in T)$ be a stochastic process and $T \subset \mathbb{R}$ be an interval. X is said to have stationary increments if

$$X_t - X_s \stackrel{d}{\rightarrow} X_{t+h} - X_{s+h}, \quad (2.1)$$

i.e., $X_t - X_s$ it has equal distribution that $X_{t+h} - X_{s+h}$, for all $s, t \in T$ and h with $t+h, s+h \in T$ (see Mikosch (1999)).

Definition 26. X is said to have independent increments if for every choice of $t_i \in T$ with $t_1 < \dots < t_n$ and $n \geq 1$, $X_{t_2} - X_{t_1}, \dots, X_{t_n} - X_{t_{n-1}}$ are independent random variables (see Mikosch (1999)).

The advantage of the BM is the postulate of independence between increments, however, this condition is not accomplished in some real situations and it is necessary to use other theoretical elements. For example, the FBM regard other assumptions, e.g. the long memory.

2.3 Fractional Brownian motion

Definition 27. According to Shevchenko (2014), a FBM is a centered Gaussian process B_t^H , with $t \geq 0$ and the covariance function

$$E(B_t^H, B_s^H) = \frac{1}{2} (t^{2H} + s^{2H} - |t - s|^{2H}). \quad (2.2)$$

where $H \in (0, 1)$ and is called the Hurst parameter.

Then, there is several properties which can be deduced immediately from the definition: stationary increments, self-similarity and dependence on the increments.

Definition 28. According to Beran et al. (2013), a stochastic process $X(t)$, with $t \in \mathbb{R}$ is called self-similar with selfsimilarity $0 < H < 1$ if for all $c > 0$, we have

$$X(ct) \stackrel{d}{=} c^H X(t) \quad (2.3)$$

where $\stackrel{d}{=}$ denotes equality in distribution.

It is important to stand out in (2.2) that

$$E [(B_{t_1}^H - B_{s_1}^H)(B_{t_2}^H - B_{s_2}^H)] < 0, \text{ for } H \in (0, 1/2) \quad (2.4)$$

and

$$E [(B_{t_1}^H - B_{s_1}^H)(B_{t_2}^H - B_{s_2}^H)] > 0, \text{ for } H \in (1/2, 1). \quad (2.5)$$

Thus, for $H \in (0, 1/2)$, the FBM has the property of counterpersistence: if it was increasing in the past, it decrease in the future, and viceversa. In contrast, for $H \in (1/2, 1)$, the FBM is persistent, and hold the trend. Moreover, for such H , the FBM has the property of long memory (long-range depece). When $H = \frac{1}{2}$ the FBM has a behaviour of a standard BM, and the covariance between two different equidistant time periods is zero (see Shevchenko (2014)).

2.4 Hurst parameter estimation

It is important to know that the parameter H can only be estimated and is not possible to determine its exact value, almost it can be was simulated. However, in literature exists several methods for its estimation (see Kirichenko et al. (2011), Bahamonde (2014) and Kaplan (2013)).

Kirichenko et al. (2011) presented a comparative analysis of the statistical properties of the H exponent estimators obtained by different methods using stationary and non-stationary fractal time series. Kirichenko et al. (2011) explained the most commonly used methods for estimating the H exponent: R/S-analysis, variance-time analysis, detrended fluctuation analysis (DFA) and wavelet-based estimation. Bahamonde (2014) presented some methods for estimating H and compared three different methodologies. Kaplan (2013) also presented different forms of estimating the H parameter and proposed its usefulness in financial markets. He illustrated an hypothesis commonly used in financial markets: “a time series that presents long-term dependence, has memory and can be considered as a series that has cyclical but not periodic patterns”. However, it is important to clarify that there are a large number of hypotheses that are commonly used in financial markets.

In addition, there are several authors who propose strategies for the estimation of H , however, it is advisable before its estimation to analyze the autocorrelation function because it gives us an approximation about the memory of the process.

2.5 Autocorrelation function

The autocorrelation function for a time series that has a long memory is

$$p(K) = Ck^{-\alpha}, \quad (2.6)$$

where $H = 1 - \frac{\alpha}{2}$, i.e. $p(K) = Ck^{-2(1-H)}$. When $H = 0.5$, we have the BM, that is, there is no correlation between the values observed in the series. When $0.5 < H < 1$, there is a positive autocorrelation, that is, the time series is persistent. Conversely, when $0 < H < 0.5$, there is negative autocorrelation, that is, the time series is antipersistent (see Kaplan (2013)).

The underlying objective of this research is to analyze the nature of the stochastic process associated with the time series and estimate the values of H in each of the trajectories of the process.

In the next chapters, the DWT is considered to estimate H and explained in more detail.

2.6 Hurst parameter in Finance

In the financial area, there are situations where returns illustrate dependence; i.e. a return value at time t may depend on a return value at time $t - 1$ or $t + 1$ in long or short periods of time.

The dependence between returns plays an essential role in the analysis of the stochastic process. For this reason, it is important to estimate the memory of the process; which is reflected in the value of H . Higher values of H , produces a stronger trend of time series.

Qian and Rasheed (2004) analyze the H exponent for trading-day periods of the Dow-Jones index. Qian and Rasheed (2004) find that the periods with large H exponents can be predicted more accurately than those with H values close to random time series. This suggests that stock markets are not totally random in all periods. Some periods have strong trend structure and this structure can be estimated by neural networks that can be useful to forecasting.

Therefore, H is a measure of how predictable the time series can be in terms of its trend. Since the upward or downward trend of financial returns provides great information on the behavior of economic variables, knowing the trend allows investors to have more information for decision making. However, we must be careful with the analysis of the trend, some investors declare that buying on the upside generates better results in terms of risk and volatility; this is only valid in short and medium time horizons. In addition, for longer time horizons, it is not advisable to give a conclusion regarding investing or buying assets with an upward or downward trend.

Another significant aspect regarding H has to do with the time horizon. It is possible to estimate its value (weekly, monthly, annually, etc), making the comment that it varies in correspondence with the temporary window. For example, in a monthly time series with measurements by second, it is possible to calculate H for all month or each of the weeks. However, these values oscillate in correspondence with the time interval.

In this thesis we not only considered the estimation of H , we also use two lines to analyze the nature of the stochastic process of the financial time series. Initially, in Chapter 3 we set time intervals, that is, we extract different subsamples of the process and we construct the 2-dimensional copula for each subsample. Subsequently, in Chapter 4 we analyze the memory of each of the time series and the cross-covariance between increments.

Chapter 3

Time copulas evolution

The daily exchange of currencies considers a high monetary flow and a large number of transactions. For this reason, it is relevant to analyze their behavior and implications in the economic development of the countries.

In this chapter, we study the process of construction of copulas for the CHFJPY and EUROJPY and we consider the time evolution of copulas is well visible in such a dynamical market as FX. We first show how several families of copulas evolving in the time for CHFJPY and EUROJPY at FX market. Black-Scholes paradigm suggest to apply evolution of copulas with respect to heat equation (see Ishimura (2014)). Stationary limit of such evolution is proven to be an independent copula under strong regularity conditions. However, empirical observations of FX stock confirm that reality can be more delicate, given by the FX market violations. We show that under slight changes of topology, the limiting object is not a copula, because the 1-Lipschitzianity continuity is violated (see Kupka et al. (2018)).

We apply this topic to the time series of the value of the currencies in each second of the interval 18:31:00 - 19:02:00 hours (january 15, 2015) in the Japanese Bank, as illustrated in the Fig. 3.1.

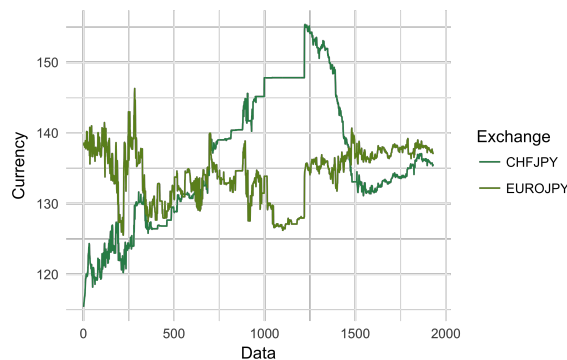


Fig. 3.1 Time series of the CHFJPY and the EUROJPY.

3.1 FX market

Conversion between currencies varies constantly in correspondence with the financial market and some economic variables: inflation, deflation, GDP, among others. This conversion is greatly influenced by: the country, the resources, the economy, the currency of these countries. This conversion greatly affects government and business decisions.

While it is true that the US dollar significantly influences the market, there are other currencies, such as: the EUR, the JPY, the GBP and the CHF, that significantly affect the market. For this reason, the relationship between currencies, becomes relevant when we analyze the dependence that emerges of them.

To analyze the dependence between currencies, it is advisable to perform an initial analysis of the percentage variation or returns. The advantage lies in the possibility of visualizing what happens with these measures at a given moment in correspondence with the past and the present value of the time series.

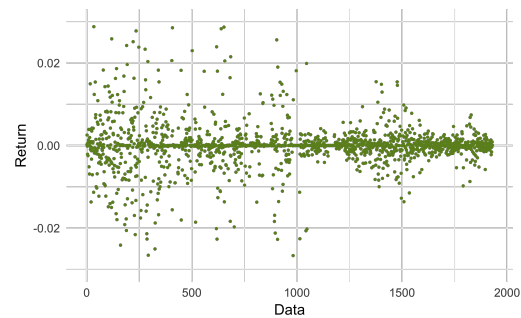
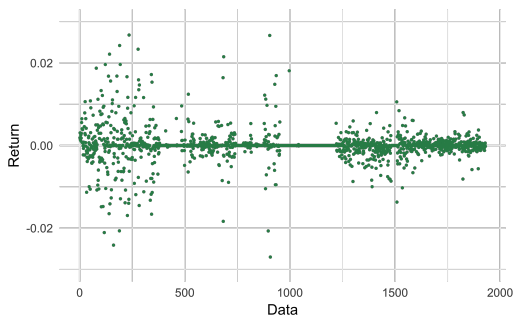


Fig. 3.2 Time series of the return CHFJPY. Fig. 3.3 Time series of the return EUROJPY.

The returns for the two currencies (see Fig. 3.2 and Fig. 3.3) are around to zero, which indicates a small variation of the present value with respect to the past one. However, in the FX market these small changes involve large amounts of money and making relevant decisions. That is, the FX market affects commercial operations between companies and governments.

3.2 Methods of constructing copulas

Fig. 3.2 and Fig. 3.3 explain the individual behavior of the returns from the currencies CHFJPY and EUROJPY, respectively. However, it is interesting to observe the relationship that exists between both currencies through the construction of 2-dimensional copulas.

A possible way to construct 2-dimensional copulas involves the extraction of different samples from the time series. Specifically, of the CHFJPY and EUROJPY currencies, we consider samples with overlapping temporary windows. Subsequently, we constructed the 2-dimensional copulas for each sample through the parametric method ML.

Definition 29. *The function*

$$c(F(x), G(y)) = \frac{\partial^2(C(F(x), G(y)))}{\partial F(x)\partial G(y)} \quad (3.1)$$

is the second mixed partial derivative of the copula C , and c is the copula density in the case that X and Y are continuous random variables.

Now, adapting the (3.1) and (1.12) for the 2-dimensional case we obtain

$$h(x, y) = c(F(x), G(y))f(x)g(y). \quad (3.2)$$

According to Manner (2007), let $\boldsymbol{\theta} \in \Theta$ be the parameter vector to be estimated by Maximum Likelihood (ML). This parameter vector can be split into the parameters for the marginals and the copula function as $\boldsymbol{\theta} = [\boldsymbol{\varphi}, \boldsymbol{\gamma}, \boldsymbol{\delta}]^T$. $\boldsymbol{\varphi} \in \Phi$ denotes the parameter(s) of $f(x)$, $\boldsymbol{\gamma} \in \Gamma$ denotes the parameter(s) of $g(y)$, and $\boldsymbol{\delta} \in \Delta$ denotes the parameter(s) of $c(F(x), G(y))$. Assume we observe a sample x_t and y_t for $t = 1, \dots, T$. The representation in (3.2) and the resulting log-likelihood function are

$$L(\boldsymbol{\theta}; \mathbf{x}, \mathbf{y}) = \prod_{t=1}^T h(x_t, y_t), \quad (3.3)$$

i.e.,

$$l(\boldsymbol{\theta}) = \ln \prod_{t=1}^T h(x_t, y_t) = \sum_{t=1}^T \ln [c(F(x_t), G(y_t))f(x_t)g(y_t)], \quad (3.4)$$

$$l(\boldsymbol{\theta}) = \sum_{t=1}^T \ln f(x_t; \boldsymbol{\varphi}) + \sum_{t=1}^T \ln g(y_t; \boldsymbol{\gamma}) + \sum_{t=1}^T \ln(c(F(x_t; \boldsymbol{\varphi}), G(y_t; \boldsymbol{\gamma})); \boldsymbol{\delta}), \quad (3.5)$$

and

$$\hat{\boldsymbol{\theta}}_{MLE} = \operatorname{argmax} \boldsymbol{\theta} \in \Theta \{l(\boldsymbol{\theta})\}. \quad (3.6)$$

This estimator is efficient as it attains the minimum asymptotic variance bound when the amount of data available for the two series are equal. However, it may be computationally difficult to obtain these estimates (see Manner (2007)).

3.3 Time evolutions of copulas and FX markets

Dependence between exchange rates, such as JPY against CHF and JPY against EUR, is an important topic. One of the most important issues is to study of time evolution of dependence structures. Accordingly, it is essential to recognize the components and correctly estimate the parameters of dependence structures in correspondence with the topological space associated with the time series. Commonly, we can find short memory models, such as: AR, MA and ARMA (see Brockwell and Davis (1991)), and long memory models, such as ARFIMA (see Granger and Joyeux (1980)). In the present work, we study the time evolutions of copulas applied to FX market. In particular, we study the time evolution of copulas and their limits with respect dynamical financial environments of nowadays economics. Following Sklar (1959) (see theorem 1.3), $Ran(F) \times Ran(G)$ captures the dependence between X and Y , and $H(x, y)$ is joint distribution function. However, copula uniqueness substantially relates also to a topological properties of underling spaces (see Stehlik (2016) and Kupka et al. (2018)).

Copulas are used to analyze bivariate functions with given marginals, and are 1-Lipschitz aggregation functions. Both aggregation functions and 1-Lipschitz aggregation functions can be defined as pure topological objects (see Stehlik (2016) and the references therein). Scarsini (1989) proved an analogous result for any probability measure in Polish (a separable completely metrizable topological space) product space. It is natural that in topologies with less regular conditions, greater is the number of additional assumptions that are required for the uniqueness of the copula representation. When we consider the support to be a product of Polish metric spaces, we need more than a strong richness in the increasing family \mathcal{A} of Borel sets, and an additional topological condition $P(\partial A) = 0$, $\forall A \in \mathcal{A}$ should be satisfied (see Scarsini (1989) and Kupka et al. (2018)).

In finance, typical sets related to trades can be very erratic and such copulas can have non-trivial supports, like fractals. We could refer to typical sets to trade that can have non-trivial supports, however for normed spaces, the new notion of the Hausdorff dimension is equivalent to the classical notion (see Definition 2) (see Kupka et al. (2018)).

3.4 1-Lipschitzian

It is clear that subcopula is a topological aggregation function according to Definition 1 in Stehlik (2016). Therein several results on the convergence of aggregation operators are given. It is clear that when topologies are not strong, Lipschitzian constant of the limit can increase (here we consider topological Lipschitzianity of Kupka (2008)). In the case of metric space, pointwise convergence preserves both 1-Lipschitzianity and associativity properties

(see Klement et al. (2001)). When target space $[0,1]$ has standard Euclidean topology, the Definition 2 will be a 1-Lipschitzian function (see Kupka et al. (2018)).

In this thesis we study convergences according to heat equation of Black and Scholes (1973). Ishimura (2014) (motivated by Black-Scholes) considers a time parametrized family of copulas. For $\forall (u, v) \in \mathbf{I}^2 : C(u, v, 0) = C_0(u, v)$

$$\frac{\partial C}{\partial t}(u, v, t) = \left(\frac{\partial^2}{\partial u^2} + \frac{\partial^2}{\partial v^2} \right) C(u, v, t), \quad (3.7)$$

$$\forall (u, v, t) \in \mathbf{I}^2 \times (0, \infty).$$

The stationary solution $C(u, v, t)$ for $t \rightarrow \infty$ is a Harmonic copula and is uniquely determined as Independent copula of the form $\Pi(u, v) = uv$. Also, the convergence is uniform. We check by computational simulation with real time data that FX evolutions can violate the type of convergence theoretically considered in Ishimura (2014), e.g., independence and 1-Lipschitz for $t \rightarrow \infty$ also a convergence of Kendall's *tau* value. As we can see in the FX stocks, many violations can happen, e.g., because of various applications of ForeX Regulation Acts in the countries (see Kupka et al. (2018)).

The specification of currency movements is of a complex nature, since significant movements and fluctuations depend on central banks, international trade and political actions in each country. If a country experiencing unfavorable conditions, its currency is likely to lose value in comparison with other countries. Therefore, investors make estimates to operate when the country recovers in order to seek for the currency to rise and make a profit. However, these estimates are generally not accurate and are affected by inexperience about the fluctuation and volatility of the time series. Consequently, continued violations of the FX market can lead to losses, which in some cases are irreparable. For example, "is the leverage effect a feature of the currency markets that adopt a floating exchange rate regime?". According to Maya and Gómez (2008), it is not always possible, the response of exchange rates to volatility shocks is characterized by memory and symmetry (for robust testing of normality and particularly symmetry see also Richter et al. (2017)); and this aspect is repeatedly overlooked (see Kupka et al. (2018)).

In the next section, we illustrate that not every evolution of copulas, which evolves according to Euclidean topology goes in weaker topology to a 1-Lipschitz aggregation operator, i.e., limit is not necessarily a copula. Here, we point out that our results are more general, i.e., they are correct also for quasi-copulas and monotonic functions with neutral element 1 (see Kupka et al. (2018)).

3.5 FX illustration of copula evolution

Time evolution of copulas plays an essential role in financial markets, specifically in the analysis of the probability function of returns. For this reason, it is necessary to estimate the copula in versatile form and to consider the dynamic structure implicit in the data. In this regard, De Mello Junior et al. (2016) propose the method EDAs (Estimation of Distribution Algorithms). De Mello Junior et al. (2016) exclaim that constant parameters are commonly used and that lead to unreliable convergences. For this reason they propose an algorithm based on numerical optimization for elliptic copulas, where the parameters of the copulas are not constant. The estimation of the dynamic structure of the parameters is made using the dependence measures, in such a way that the convergence of the copula sequence is nearest to the real copula (see Kupka et al. (2018)).

For this reason, this thesis focuses on the dynamic structure of the data, in such a way that the parameters of the copula are not fixed and evolve in time according to the time interval. Notice that the theoretical version of Kendall's τ for copula C_t is given by (1.20). Here we have to point out that the convergence of time τ can be drastically influenced by the measure $dC(u, v)$. Clearly $\tau_{\Pi} = 0$ and, in Ishimura and Yoshizawa's (2011) is shown for (3.7) that Kendall's τ (and also Spearman's ρ) converges to zero exponentially as $t \rightarrow \infty$. But the empirical results shows something different. The problem is that integral representations of τ hold only for copulas.

In this thesis, we consider 1000 overlapped samples and construct the 2-dimensional copula for each of them. In order to illustrate this in a real data example, we work with Japanese Bank trading data from 2015. The database contains the variables: time (hour-minutes-seconds) for CHFJPY ratio, EUROJPY ratio and EURO/CHF.

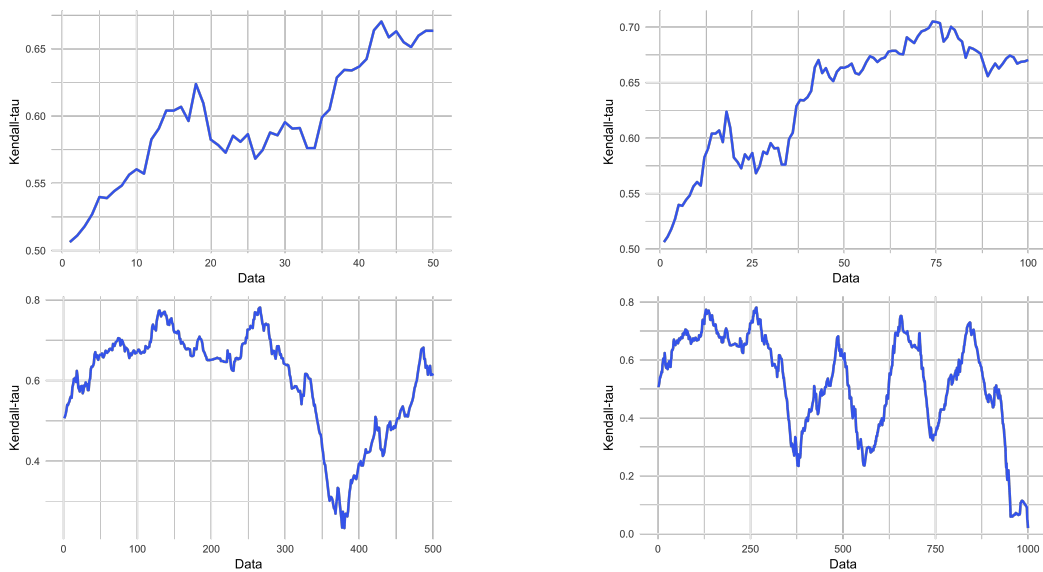
Using R software (R Core (2014)), along with packages: copula, VineCopula, MASS, rgl, readr, fCopulae, ggplot2, dplyr, PerformanceAnalytics, urca, MASS, tseries, scales, psych and PerformanceAnalytics, we generating a data set containing the value per second for each of the: CHFJPY, EUROJPY and EURO/CHF. Subsequently, we constructed the empirical copulas through the function BiCopSelect, obtaining the outputs: family, pair, par2, tau, emptau, cor, among others. The construction of empirical copulas was performed for different data sets considering the evolution in time, this is, all the sets began with the observations 1-100 and increased in the time.

The construction of empirical copulas was performed for data sets as illustrated on Table 3.1.

We illustrate the value of empirical Kendall's τ for 50, 100, 500 and 1000 groups in the Fig. 3.4.

Data	Total	Data	Total	Data	Total	Data	Total
1-100	100	1-100	100	1-100	100	1-100	100
2-101	100	2-101	100	2-101	100	2-101	100
3-102	100	3-102	100	3-102	100	3-102	100
4-103	100	4-103	100	4-103	100	4-103	100
⋮	⋮	⋮	⋮	⋮	⋮	⋮	⋮
50-149	100	100-199	100	500-599	100	1000-1099	100

Table 3.1 Total data for 50, 100, 500 and 1000 groups.

Fig. 3.4 Kendall's τ (50, 100, 500 and 1000 samples).

Observing the behavior of the different groups in each of the experiments, we found the different copulas when a change in the time interval is generated. In Fig. 3.5, we can observe the time evolution of parameters of copulas. For example, for the first 10 groups we get the evolution displayed on Table 3.2.

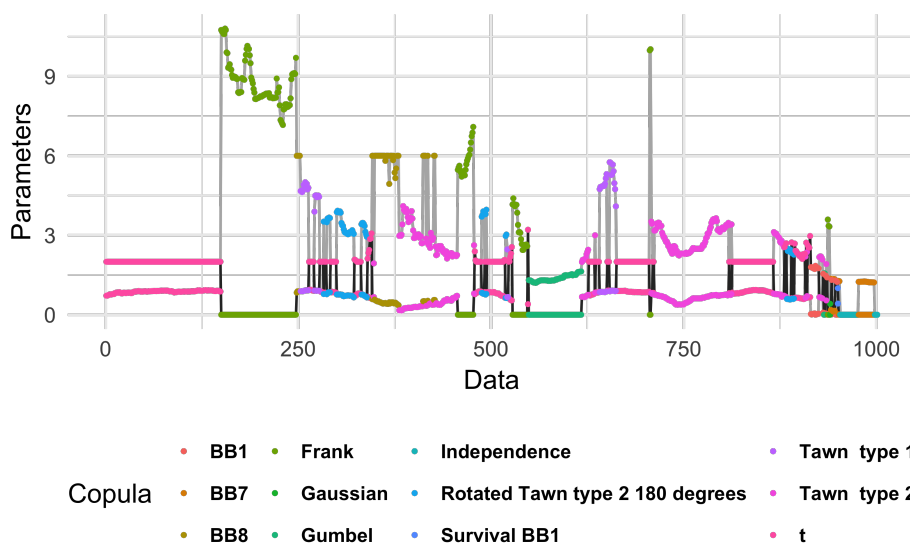


Fig. 3.5 Graphical illustration of time evolution of parameters in the copulas.

Family	Par	Par 2
2	0.7187821	2.0001
2	0.7236032	2.0001
2	0.7318585	2.0001
2	0.7496528	2.0001
2	0.7661419	2.0001
2	0.7616225	2.0001
2	0.7675449	2.0001
2	0.7705791	2.0001
2	0.780207	2.0001
2	0.7841979	2.0001

Table 3.2 Evolution of parameters of copulas for the first 10 groups.

Fig. 3.5 shown that there is no specific pattern for the parameters of the copulas constructed. However, there are copulas groups that correspond to the same family and where the parameter changes.

Considering all the groups which appeared in simulations, the resulting empirical copulas are illustrated in Table 3.3.

Copula	Software output	Frequency
BB1	7	18
BB7	9	28
BB8	10	46
Frank	5	144
Gaussian	1	1
Gumbel	4	71
Independence	0	27
Rot Tawn 2 180 deg.	214	54
Survival BB1	17	1
Tawn 1	104	39
Tawn 2	204	206
t	2	365

Table 3.3 Frequency of the copulas in the samples.

The copulas that are obtained more often in the samples are: t-student, Tawn 2 and Frank. The Tawn copula correspond to the Archimedean family, and the t-student copula to the elliptical family and the extreme value copulas.

The t-student copula predominates in the 1000 samples extracted from the data set, that is, there are financial events where the returns are not characterized Gaussian distribution. For example, the non-Gaussian of the returns leads to the impossibility of using the theory exposed by Markowitz in the construction of Portfolios. In Chapter 4 we will deal with this issue in more detail.

According to Genest et al. (2011), the symmetric extreme-value copulas are: the Gumbel–Hougaard (GH), Galambos (GA), Hüsler–Reiss (HR) and Student extreme-value (t-EV) copula with four degrees of freedom; and the asymmetric extreme-value copulas are: asymmetric versions of the Gumbel–Hougaard (a-GH), Galambos (a-GA), Hüsler–Reiss (a-HR), and Student extreme-value (a-t-EV) copula with four degrees of freedom.

In this thesis we focus on the t-student because it is the most frequent copula among the samples. Samples with copula t-student are: 1-149, 264-270, 278-282, 284-286, 292-299, 323-331, 340-345, 214, 479-487, 492, 495-518, 523-527, 548, 627-634, 636-640, 651-653, 663-705, 710-711, 809, 813-866, 881, 883, 890, 894-907, 909 and 911-914.

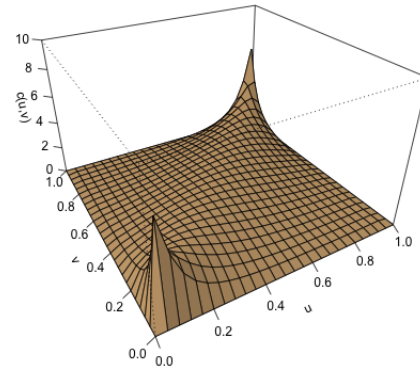
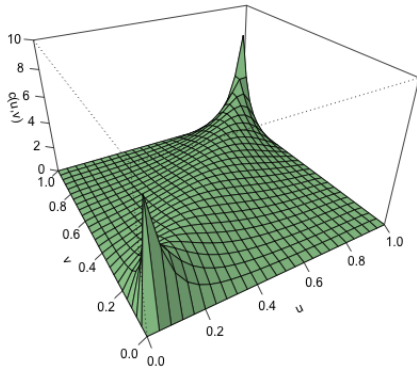


Fig. 3.6 d-copula t-student for the 5 sample. Fig. 3.7 d-copula t-student for the 548 sample.

Fig. 3.6 and Fig. 3.7 shown that the relationship between currencies concentrates values at the extremes making the tails are the high correlation between both currencies.

3.6 Dependence measures

In Fig. 3.4, we observe the empirical Kendall's τ values for 50, 100, 500 and 1000 groups. Remember that the association measures us possible to evaluate the linear or non-linear relationship between two or more variables. For example, the Pearson correlation coefficient is a measure of the linear association between the variables; covariance is a measure of joint variability; and the Kendall's τ coefficient value, measures the not necessarily linear association between the measured quantities.

In this thesis we rely on Theorems 8, 9 and 10 in the framework of the theory of copulas. For the 1000 samples, we determine the coefficients τ and ρ , together with the upper and lower bounds that link both measures, according to the Theorem 10.

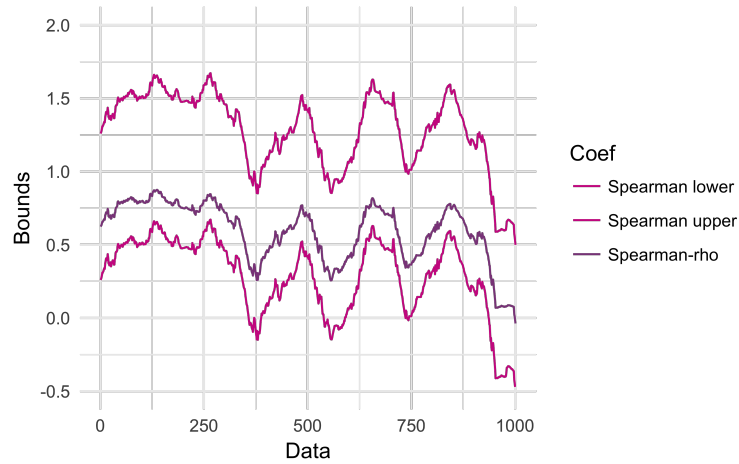


Fig. 3.8 Upper and lower bounds for Spearman's ρ coefficient.

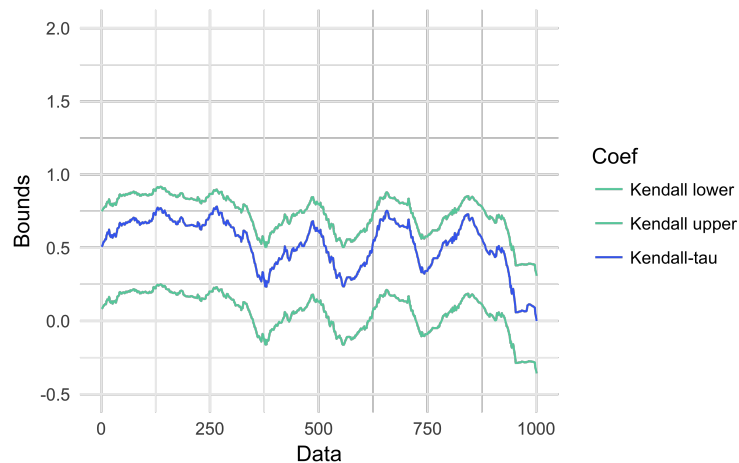


Fig. 3.9 Upper and lower bounds for Kendall's τ coefficient.

We observed in Figures 3.8 and 3.9 that τ and ρ vary in correspondence with the sample; i.e., it can not be assured if the return of the CHFJPY increases, the returns of the EUROJPY also. Similarly, it can not be assured if the return of the CHFJPY and EUROJPY decreases, the return of the EUROJPY also.

The financial time series of the FX market are characterized by its versatility, specifically by its volatility, an aspect frequently used to quantify risk. Volatility is a measure of the frequency and intensity of changes in the price of an asset (currency) in a specific time horizon, which is defined as the standard deviation of that change.

With the results obtained, we can conclude that

$$\lim_{S_t \rightarrow \infty^+} C_{S_t}(u, v) \text{ is divergent,} \quad (3.8)$$

where S_t it is the number of samples, $C_{S_t}(u, v)$ is the copula for each of the samples, u is the CDF for the currency 1, and v the CDF for the currency 2.

Additionally, we conclude that

$$\lim_{S_t \rightarrow \infty^+} \tau_{S_t}(u, v) \text{ is divergent,} \quad (3.9)$$

where τ_{S_t} is Kendall's *tau* value in each one of the samples of the $C_{S_t}(u, v)$.

3.7 Copulas observed in FX data

In this section we illustrate both qualitative changes in type of copulas (see Table 3.3) and changes in parameters for a given copula families (see Table 3.2, Fig. 3.5). Next, we describe several copulas involved in FX data (see Kupka et al. (2018)).

3.7.1 t-student Copula

This copula remains is invariant under a standardization of the marginal distributions (in fact, is invariant under any series of strictly increasing transformations of the components of the random vector \mathbf{X}). This means that the copula of a $t_d(v, \boldsymbol{\mu}, \Sigma)$ is identical to that of $t_d(v, \mathbf{0}, P)$ distribution, where P is the correlation matrix related to the dispersion matrix Σ . The t copula is thus given by

$$C_{v,P}^t(u) = \int_{-\infty}^{t_v^{-1}(u_1)} \cdots \int_{-\infty}^{t_v^{-1}(u_d)} \frac{\Gamma(\frac{v+d}{2})}{\Gamma(\frac{v}{2})\sqrt{(\pi v)^d |P|}} \left(1 + \frac{x^T P^{-1} x}{v}\right)^{-\frac{v+d}{2}} dx, \quad (3.10)$$

where t_v^{-1} denotes the quantile function of a standard univariate t_v distribution. In the bivariate case, we simplify the notation to $C_{v,\rho}^t$, where ρ is the off-diagonal element of P (see Demarta and J. McNeil (2004)).

3.7.2 Tawn Copula

The Tawn copula is an asymmetric extreme value copula, which is an extension of the Gumbel copula. It has the following dependence function

$$A(t) = 1 - \beta + (\beta - \alpha)t + [\alpha^r + t^r + \beta^r(1-t)^r]^{\frac{1}{r}}, \quad (3.11)$$

where $0 \leq \alpha, \beta \leq 1$ and $r \geq 1$ (see Mendes et al. (2007)).

3.7.3 Gumbel Copula

The dependence function of Gumbel copula is

$$C_{\theta}(u, v) = u + v - 1 + (1 - u)(1 - v) \exp^{\theta \ln(1-u) \ln(1-v)}, \quad (3.12)$$

where θ is a parameter in $[0, 1]$ and the marginal distribution functions are exponentials, with quasi-inverses $F^{-1}(u) = -\ln(1 - u)$ and $G^{-1}(v) = -\ln(1 - v)$ for u, v in \mathbf{I} (see Nelsen (2006)).

3.7.4 Frank Copula

The Frank copula is an Archimedean copula with the following distribution function

$$C_{Fra}^{\delta}(u, v) = -\delta^{-1} \left(\frac{\eta - (1 - e^{\delta u})(1 - e^{\delta v})}{\eta} \right), \quad (3.13)$$

where $\delta > 0$ and $\eta = 1 - e^{\delta}$ (see Mendes et al. (2007)).

3.7.5 Archimedean Copula

Let φ be a continuous, strictly decreasing function from \mathbf{I} to $[0, \infty]$ such that $\varphi(1) = 0$, and let $\varphi^{[-1]}$ be the pseudo-inverse of φ . Let C be the function from \mathbf{I}^2 to \mathbf{I} given by

$$C(u, v) = \varphi^{[-1]}(\varphi(u) + \varphi(v)). \quad (3.14)$$

C satisfies the boundary conditions for a copula and the the function φ is called a generator of the copula (see Nelsen (2006)).

3.7.6 Family BB8 Copula

A family of copulas based on a two-parameter family of LTs (Laplace transformations),

$$\phi(s; \theta, \delta) = \delta^{-1} \left[1 - \left\{ 1 - [1 - (1 - \delta)^{\theta}] \exp^{-s} \right\}^{\frac{1}{\delta}} \right], \quad \theta \geq 1, 0 < \delta \leq 1, \text{ is}$$

$$C(u, v; \theta, \delta) = \delta^{-1} \left[1 - \left\{ 1 - [1 - (1 - \delta)^{\theta}]^{-1} [1 - (1 - \delta u)^{\theta}] [1 - (1 - \delta v)^{\theta}] \right\}^{\frac{1}{\delta}} \right] \quad (3.15)$$

where $\theta \geq 1, 0 \leq \delta \leq 1$ (see Joe (1997)).

In the construction of 2-dimensional copulas, is fundamental to recognize the intrinsic nature of time series associated with the stochastic process. Under specific conditions on each of the samples, we find that the copula sequence does not converge to product copula. Moreover, we can conclude that the time evolution in correspondence with the lag of both time series, CHFJPY and EUROJPY, leads to different copulas according to the Kendall's τ value in the copulas sequence.

In the next chapter, we expose the intrinsic nature of the data set and the characteristics of the stochastic process, in correspondence with the process memory.

Chapter 4

Assessment of long memory in non-Gaussian process using copulas

In this chapter, we constructed the TCLM model using the t-student copula and Gaussian bivariate distribution. We estimated the H exponents in each trajectory of the stochastic bivariate process, and finally, we calculate the cross-covariance between increments.

4.1 Degrees of freedom parameter in the t-student distribution and bivariate Gaussian process

According to Demarta and J. McNeil (2004), the d -dimensional random vector $X = (X_1, \dots, X_d)'$ is said to have a (non-singular) multivariate t distribution with ν degrees of freedom, mean vector $\boldsymbol{\mu}$ and positive-definite dispersion or scatter matrix Σ , denoted $\mathbf{X} \sim t_d(\nu, \boldsymbol{\mu}, \Sigma)$, if its density is given by

$$f(\mathbf{x}) = \frac{\Gamma(\frac{\nu+d}{2})}{\Gamma(\frac{\nu}{2})\sqrt{(\pi\nu)^d|\Sigma|}} \left(1 + \frac{(\mathbf{x} - \boldsymbol{\mu})'\Sigma^{-1}(\mathbf{x} - \boldsymbol{\mu})}{\nu}\right)^{-\frac{\nu+d}{2}}. \quad (4.1)$$

Note that in this standard parameterization $cov(\mathbf{X}) = \frac{\nu}{\nu-2}(\Sigma)$, so that the covariance matrix is not equal to Σ and is in fact only defined if $\nu > 2$.

Now, using the R software (R Core (2014)) along with packages: copula, MASS, psych, rgl, VineCopula, readr, PerformanceAnalytics, wavelets, ggplot2, mvtnorm, scatterplot3d, plot3D and hypergeo; we calculate the outputs: τ , ρ and λ .

According to Demarta and J. McNeil (2004), the previous values allow us to calculate $\hat{\nu}$ for the bivariate process using

$$\lambda = \frac{\int_{(\frac{\pi}{2}-\arcsin(\rho))/2}^{\frac{\pi}{2}} \cos^{\alpha} t dt}{\int_0^{\frac{\pi}{2}} \cos^{\alpha} t dt}, \quad (4.2)$$

for the 2-dimensional t-student, $\alpha = \nu$.

Thus, to obtain $\hat{\nu}$ from the bivariate process we initially used the ML method to estimate the parameters of the copula, and then, we determined $\hat{\nu}$ using the coefficients ρ and λ .

The $\hat{\nu}$ parameter is useful for the application of some basic theorems. For example, Demarta and J. McNeil (2004) illustrates the possibility of transforming the t-student random variable into a Gaussian by knowing in advance the degrees of freedom of the t-student.

According to Demarta and J. McNeil (2004), the random variable $X \sim t - student(\nu, \mu, \sigma^2)$ can be transformed into a random gaussian variable by a weigh that follow an inverse gamma, i.e.,

$$W^{-1}X = Z, \quad (4.3)$$

where $Z \sim N(0, \sigma^2)$, W is independent of Z and $W \sim Gamma(\nu/2, \nu/2)$.

In a multivariate Gaussian distribution, each of the marginal ones is univariate Gaussian. In addition, if the covariances are zero, the random variables are independent. In this thesis, we focus on the case where covariances are different from zero.

This is how we proceed with the extraction of univariate gaussian variables and analyze their marginal behavior. Initially, we check the: stationary increments, self-similarity and dependence among the increments. Then, we proceed with the analysis of memory. Specifically, we do the estimation of Hurst parameter for the two trajectories of the bivariate process.

4.2 Hurst parameter estimation with DWT

For the estimation of H exist different methods, such as: discrete derivative of second order, wavelets transform, rescaled range, aggregated variance, detrended fluctuation analysis, absolute moments, among others (see: Bahamonde (2014), Kaplan (2013) and Kirichenko et al. (2011)).

In particular, we use the DWT method, which consists a decomposition of two time series according to the original time series, this is, a time series with the detail coefficients ($d_{j,k}$) and other with the scale coefficients ($a_{j,k}$).

According to Abry et al. (2000), $a_{j,k}$ and $d_{j,k}$, are defined as follows:

$$a_{j,k} = \int_{-\infty}^{\infty} X(t) \phi_{j,k}(t) dt \quad (4.4)$$

and

$$d_{j,k} = \int_{-\infty}^{\infty} X(t) \psi_{(j,k)}(t) dt, \quad (4.5)$$

where $\phi_{j,k}(t) = 2^{-j/2} \phi(2^{-j}t - k)$, $\psi_{j,k} = 2^{-j/2} \psi(2^{-j}t - k)$, $\psi(t - k)$ is the translation of ψ to the right by k units, 2^j is the scale and $j, k \in \mathbb{Z}$.

Kaplan (2013) states that it is possible to obtain \hat{H} with a linear regression on the values using the expression

$$\log_2 \left(\frac{1}{n_j} \sum_{k=1}^{n_j} |d_{j,k}|^2 \right) \quad (4.6)$$

on j , where j represents the decomposition level. To calculate \hat{H} , Kaplan (2013) used the equation

$$\hat{H} = \left| \frac{\beta - 1}{2} \right|, \quad (4.7)$$

where β is the slope on the regression line on (4.6) respect to j .

4.3 Covariance function on the 2-dimensional FBM

Now, it is important to analyze what happens between the two trajectories of the process, for this, we analyze the cross-covariance between the both.

Let $X = \{X(t), t \in \mathbb{R}\}$ a 2nd order process with values in \mathbb{R}^p . Assume that X has stationary increments, zero mean, $X(0) = 0$, and that X is vector self-similar with exponent $H = \text{diag}(H_1, \dots, H_p)$, $0 < H_i < 1$, $i = 1, \dots, p$.

Moreover, assume also that for any $i, j = 1, \dots, p$, the function $t \mapsto EX_i(t)X_j(1)$ is continuously differentiable on $(0, 1) \cup (1, \infty)$. Let $\sigma_i^2 > 0$ denote the variance of $X_i(1)$, $i = 1, \dots, p$.

If $i \neq j$ and $H_i + H_j \neq 1$, then there exists $c_{ij}, c_{ji} \in \mathbb{R}$ such that for any $(s, t) \in \mathbb{R}^2$

$$\text{Cov}(X_i(s)X_j(t)) = \frac{\sigma_i \sigma_j}{2} \{c_{ij}(s)|s|^{H_i+H_j} + c_{ji}(t)|t|^{H_i+H_j} - c_{ji}(t-s)|t-s|^{H_i+H_j}\}, \quad (4.8)$$

where $\sigma_i^2 = \text{var}(X_i(1))$ (see Lavancier et al. (2009)).

With respect to $c_{ij}(t)$, Lavancier et al. (2009) asseverate that:

$$c_{ij}(t) = 2 \frac{\tilde{c}_{ij} \phi_{ij}}{\sigma_i \sigma_j} \quad (4.9)$$

and

$$\phi_{ij} = \frac{B(H_i + 0.5, H_j + 0.5)}{\sin((H_i + H_j)\pi)}, \quad (4.10)$$

where B are the Beta function.

$\tilde{C} = \tilde{c}_{ij}$ is a matrix given by

$$\tilde{C} = \cos(H\pi)A_+A_+^* + A_-A_-^*\cos(H\pi) - \sin(H\pi)A_+A_-^*\cos(H\pi) - \cos(H\pi)A_+A_-^*\sin(H\pi), \quad (4.11)$$

where A_{\pm} are real $p \times p$ matrices, A^* denotes the transposed matrix,

$\sin(H\pi) = \text{diag}(\sin(H_1\pi), \dots, \sin(H_p\pi))$ and $\cos(H\pi) = \text{diag}(\cos(H_1\pi), \dots, \cos(H_p\pi))$

(see Lavancier et al. (2009)).

Now, the cross-covariance of the increments of size δ of componentes i and j when $H_i + H_j \neq 1$ (see Amblard et al. (2010)) is given by

$$\gamma_{i,j}(h, \delta) = \mathbb{E}\Delta_{\delta}X_i(t)\Delta_{\delta}X_j(t+h) = \frac{\sigma_i\sigma_j}{2} (w_{i,j}(h-\delta) - 2w_{i,j}(h)) + (w_{i,j}(h+\delta)), \quad (4.12)$$

where

$$w_{i,j}(h) = (\rho_{i,j} - \eta_{i,j}\text{sign}(h))|h|^{H_i+H_j}. \quad (4.13)$$

and $\rho_{i,j} = (c_{i,j} + c_{j,i})/2$ and $\eta_{i,j} = (c_{i,j} - c_{j,i})/2$.

In conclusion, the coherence function between the increments of size δ between the components i and j on the 2-dimensional FBM are

$$C_{i,j}(w, \delta) = \frac{\Gamma(H_i + H_j + 1)^2}{\Gamma(2H_i + 1)\Gamma(2H_j + 1)} \frac{\rho_{i,j}^2 \sin(\frac{\pi}{2}(H_i + H_j)^2) + \eta_{i,j}^2 \cos(\frac{\pi}{2}(H_i + H_j)^2)}{\sin(\pi H_i) \sin(\pi H_j)}. \quad (4.14)$$

When $p = 2$, i.e., on the 2-dimesional case, for fixed values of H_1 and H_2 , the condition $C_{1,2} \leq 1$ means that the set of possible parameters $\rho_{1,2}$ and $\eta_{1,2}$ is inside an ellipse, i.e., it is possible to determine the maximum correlation that may exist between the increments respecto to the reseach currencies.

4.4 Construction of the TCLM model

In the context of financial time series, it is initially recommended to extract the percentage variation or returns, and then, perform the statistical treatment. The returns make it possible to visualize the behavior of the series at a specific moment in correspondence with its past or future value.

In the next steps, we expose the TCLM model as a possible way to capture the subjacent stochastic process in the dependence relation between two currencies. Initially we check the distributional assumption of the returns of both currencies using different tests. There we find that the two series do not reflect a gaussian behavior. Additionally, we constructed the 2-dimensional copula and found a copula of extreme values, t-student copula. Then, knowing the copula and its respective parameters, we proceed with the calculation of \hat{v} using (4.2); subsequently, we apply (4.3) and obtain the bivariate Gaussian distribution.

Remember that the bivariate Gaussian distribution ensure that each of the marginal ones is gaussian, allowing us to proceed with the extraction of the marginals. The great utility of univariate Gaussian densities lies in the possibility of using the basic theory of stochastic processes. However, we make the exception of the verification of the assumptions before applying any theorem.

For the time series studied, we check the assumptions of the FBM and estimate H in each of them. Then, we proceed with the reconstruction of the bivariate process using the obtained estimates (\hat{v} , \hat{H}_1 and \hat{H}_2), and finally, we calculate the coherence function between the two trajectories (\hat{H}_1 and \hat{H}_2).

In summary, Fig. 4.1 illustrates the method used for the construction of the TCLM model.

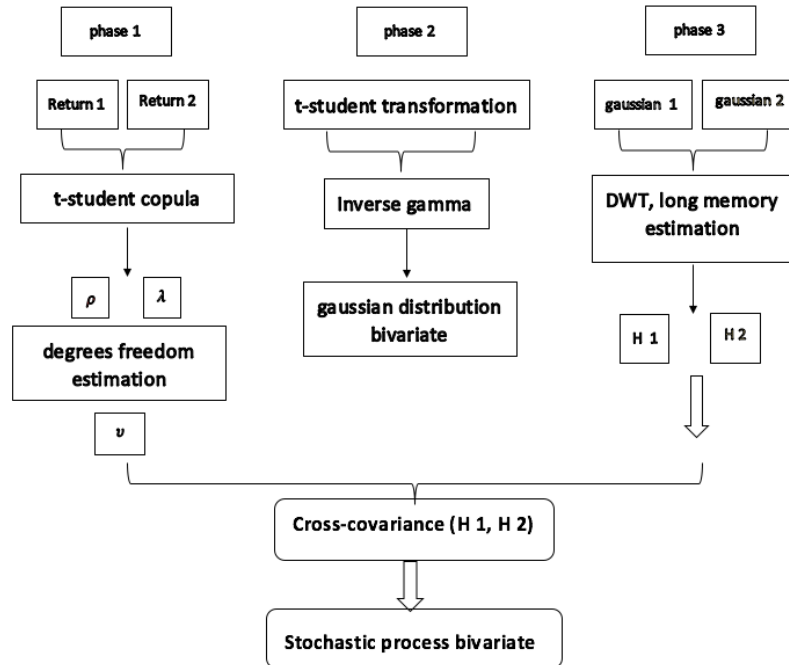


Fig. 4.1 Method construction of the TCLM model.

4.5 Non-gaussian bivariate process

It is known in the financial area that the returns of some time series do not always keep a Gaussian distribution. On repeated occasions, we can find returns that follow distributions of heavy tails; e.g., the frequency for the returns of CHFJPY and EUROJPY currencies of the Japanese Bank, together with the normality tests for each of the time series, provide evidence to ensure that the returns do not follow a Gaussian distribution (see Fig. 4.2 and Fig. 4.3).

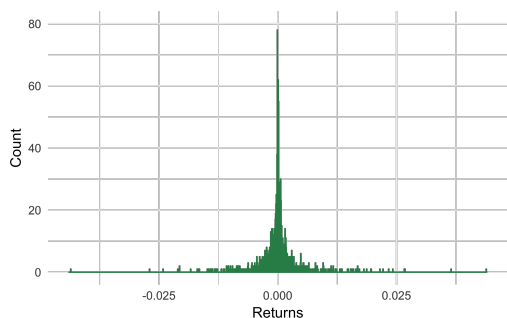


Fig. 4.2 Returns of the CHFJPY.

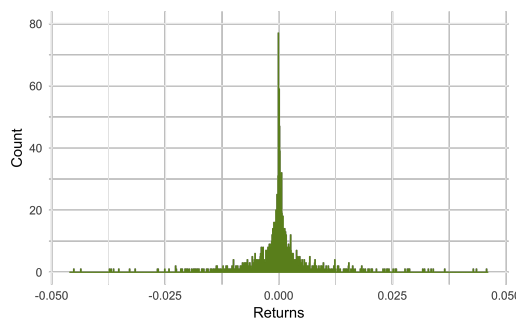


Fig. 4.3 Returns of the EUROJPY.

According with the previous results, there is a required to study the non-Gaussian returns and their implications theoretical and practical. In this regard, to recognize the distribution of the data (returns of currencies) its important by to involve understanding the implicit and explicit characteristics of the stochastic process associated to the time series. Therefore, the next ideas allow us to approach this situation.

It is important to note that Fig. 4.2 and Fig. 4.3 figures illustrate the marginal behavior of the time series, but ¿what happens with the joint behavior? (that is, with the bivariate stochastic process that involves both currencies). Now, if we construct the 2-dimensional copula with both marginals, we obtain the 2-dimensional density copula t-student as shown in Fig. 4.4. The level curves for the density of t-student copula illustrate the extreme behavior of the currencies as shown in Fig. 4.5.

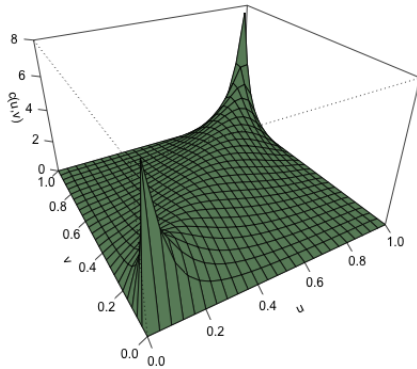


Fig. 4.4 Density t-student copula.

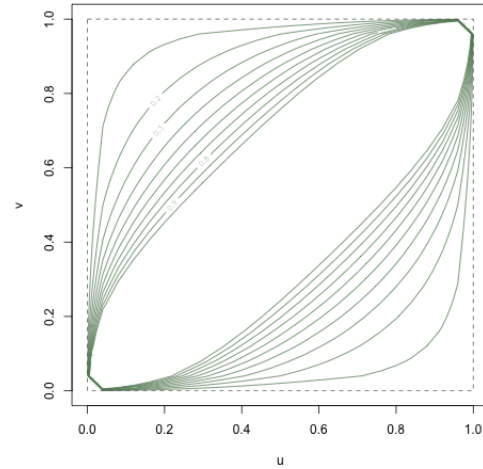


Fig. 4.5 Level curves t-student copula.

In the next subsections we will present: the process of construction of the 2-dimensional copula, the estimation of the degrees of freedom of the bivariate process using the coefficient of tails and the correlation coefficient; the transformation of the bivariate t-student random vector into bivariate Gaussian; and the cross-covariance between the increments.

4.6 Analysis data

4.6.1 Real data

In this section, we apply the TCLM model to a set of real data. The time series correspond to the trajectories presented Chapter 3 (see Fig. 3.1). Initially, we construct 2-dimensional copula as illustrated in Fig. 4.6.

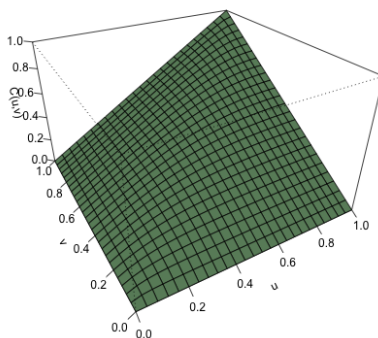


Fig. 4.6 t-student copula for the CHFJPY and EUROJPY returns.

The density associated with the copula is observed in Fig. 4.4. Knowing the copula and some measures associated with it, such as, $\rho = 0.756$ and $\lambda = 0.564$, we applying (4.2) and estimate $\hat{\nu}$ to obtain

$$\lambda = \frac{\int_0^{\frac{\pi}{2}} 0.1138\pi \cos^{\nu} t dt}{\int_0^{\frac{\pi}{2}} \cos^{\nu} t dt}. \quad (4.15)$$

We solve (4.15) and we obtain

$$\begin{aligned} 0.564 = & 2\Gamma\left(\frac{\nu}{2} + 1\right)(0.940881^{(\nu+1)})F_{2,1}\left(1/2, (\nu+1)/2; (\nu+3)/2; 0.885257\right) - \\ & (6.12323 \times 10^{(-17)})(6.12323 \times 10^{(-17\nu)})F_{2,1}\left(1/2, (\nu+1)/2; (\nu+3)/2; 3.7494 \times 10^{(-33)}\right) / \\ & (\sqrt{\pi}\Gamma((\nu+1)/2)(\nu+1)), \end{aligned} \quad (4.16)$$

where $F_{2,1}$ are the Gaussian hypergeometric function.

The convergence on (4.16) about $\hat{\nu}$ is illustrated in Fig. 4.7 .

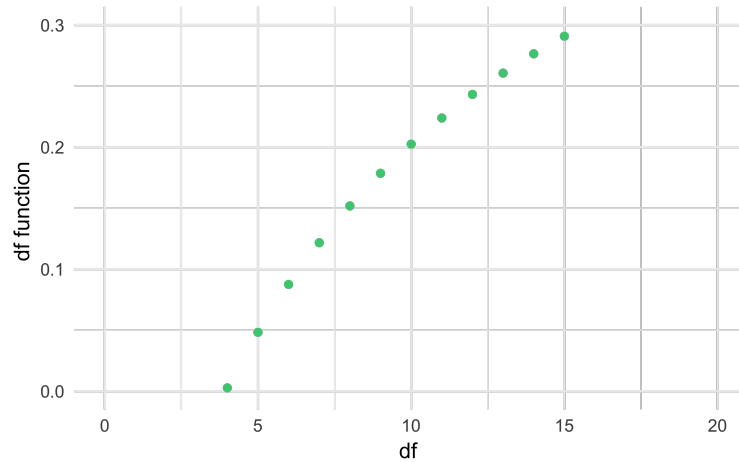


Fig. 4.7 Convergence of degrees of freedom ($\hat{\nu}$) on the t-student copula.

Now, we proceed with the generation of the gamma distribution, $gamma \sim (2, 2)$ knowing that $\hat{\nu} \approx 4$. Next, we determine its inverse and use (4.3) to construct the bivariate Gaussian distribution. Solving this allows to extract the marginal Gaussian, this case, the marginal ones for the CHFJPY and EUROJPY currencies.

For the analysis of the memory on each of the currencies; we verify the assumptions: stationary increments, self-similarity and dependence on the increments; once these assumptions are fulfilled, we proceed with the estimation of the H parameter in each trajectory.

In Subsection 2.6 we refer to the H parameter as an indicator of the memory of the process and we alluded to some existing methods for its estimation. We use the DWT method, initially we construct the regression lines for each of the currencies using the expression (4.6), and later, we estimate H parameter using (4.7).

In particular, for the returns of the CHFJPY and EUROJPY we obtain the following regression lines (see Fig. 4.8 and Fig. 4.9).

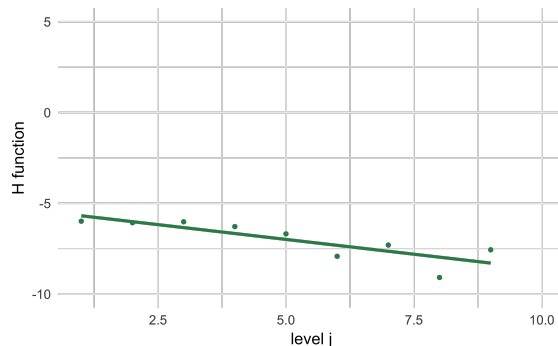


Fig. 4.8 Regression line return CHFJPY.

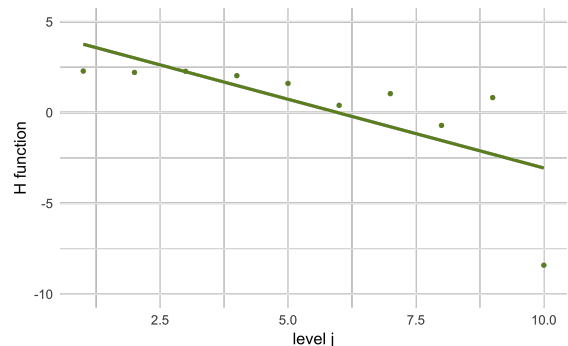


Fig. 4.9 Regression line return EUROJPY.

The regression lines equations and the values of \hat{H}_1 and \hat{H}_2 are illustrated in Table 4.1.

Serie	Regression line	\hat{H}
CHFJPY	$y = - 0.7225 j - 5.1073$	0.8613
EUROJPY	$y = - 0.7578 j + 4.5205$	0.8789

Table 4.1 \hat{H}_1 and \hat{H}_2 using DWT (real data).

Remember that \hat{H} parameter is associated with the fractal dimension and that it provides the degree of how rough the surface is for a set of self-similar increments. In particular, the bivariate stochastic process with $\hat{H}_1 = 0.8613$ and $\hat{H}_2 = 0.8789$ for the two trajectories analyzed, indicates that: there are positive correlations between the increases for each of the series, the fractal curves are softer and the observations contain long-term dependence. In addition, values of \hat{H} so close, guarantee that we are effectively focusing on the bivariate stochastic process associated with the joint behavior of currencies.

From a practical point of view, the long-term memory for the series of financial returns on the CHFJPY and the EUROJPY indicates that there is persistence, i.e., within certain periods of time, the value of the currency CHFJPY depends on the values in previous periods; in the same way it happens for the currency EUROJPY.

With both components, i.e., the marginal behavior (memory of each of the trajectories) and the bivariate behavior ($\hat{\nu}$ of the bivariate t-student copula), we proceed with the reconstruction of the 2-dimensional stochastic process. We illustrate on Fig. 4.10 an approximation to the stochastic process reconstructed.

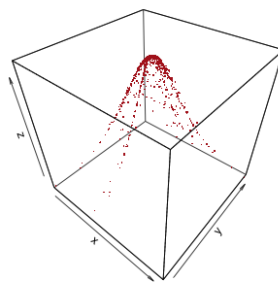


Fig. 4.10 Stochastic process reconstructed (real data).

Finally, we expose the coherence function between the increments according to (4.14) equation. When $p = 2$, i.e., on the bivariate case, for fixed values of H_1 and H_2 , the condition $C_{1,2} \leq 1$ means that the set of possible parameters $\rho_{1,2}$ and $\eta_{1,2}$ is inside an ellipse.

For the time series of the returns of the CHFJPY and EUROJPY with $\hat{H}_1 = 0.8613$ and $\hat{H}_2 = 0.8789$, we obtain the ellipse on Fig. 4.11.

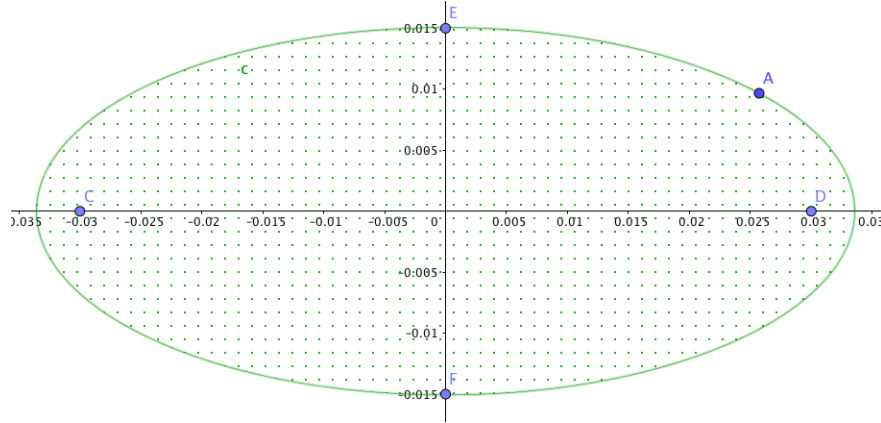


Fig. 4.11 Coherence function (ellipse on real data).

The equation on the ellipse is

$$\frac{\rho_{1,2}^2}{0.0012} + \frac{\eta_{1,2}^2}{0.00024} \leq 1. \quad (4.17)$$

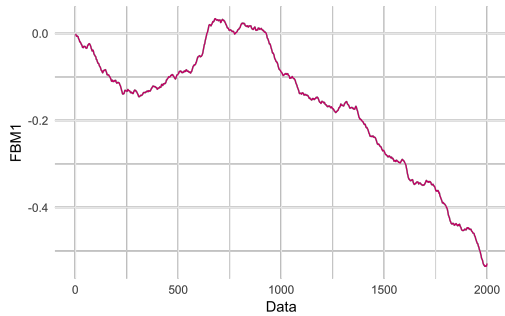
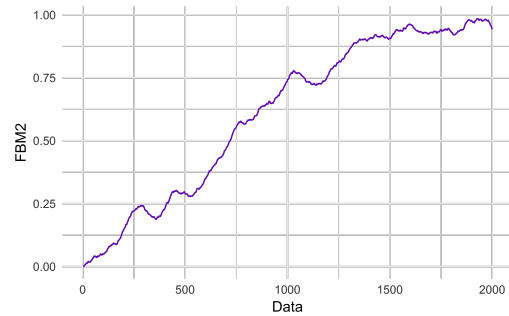
Remember that the coherence function allows us to examine the relationship between two time series. In addition, for cases in which the assumptions of the linear system are insufficient, the Cauchy-Schwarz inequality guarantees that its value is less than 1, as is our case.

4.6.2 Simulated data

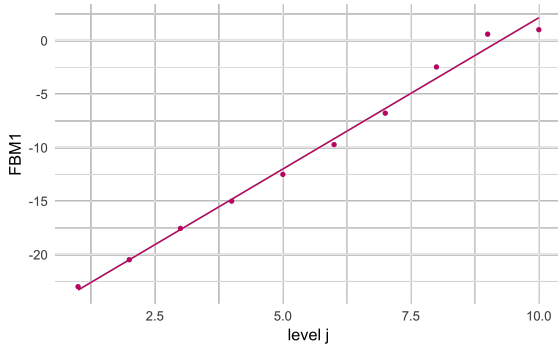
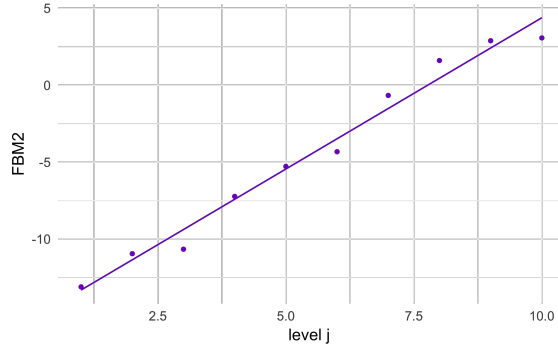
Next, we expose the application of the TCLM model on simulated data. We make the warning that we start by constructing Gaussian marginals, i.e., a FBM_1 and a FBM_2 . The Hurst parameters simulated are $H_1 = 0.89$ and $H_2 = 0.87$. Additionally, $\boldsymbol{\mu}_{2000 \times 1}^1 = \mathbf{0}$, $\boldsymbol{\Sigma}_{2000 \times 2000}^1$, $\boldsymbol{\mu}_{2000 \times 1}^2 = \mathbf{0}$ and $\boldsymbol{\Sigma}_{2000 \times 2000}^2$. Remember that $\boldsymbol{\Sigma}$ is given by (see Bahamonde (2014))

$$C(B_H(i), B_H(j)) = \frac{1}{2} \left[\left(\frac{i}{n} \right)^{2H} \left(\frac{j}{n} \right)^{2H} \right] - \left| \frac{i}{N} - \frac{j}{N} \right|^{2H}. \quad (4.18)$$

Fig. 4.12 illustrate the simulated FBM_1 and the Fig. 4.13 the simulated FBM_2 .

Fig. 4.12 FBM_1 , $H_1 = 0.89$.Fig. 4.13 FBM_2 , $H_2 = 0.87$.

We use the DWT for estimate \hat{H}_1 y \hat{H}_2 . Fig. 4.14 and Fig. 4.15 illustrate the regression lines according to (4.6).

Fig. 4.14 Regression line FBM_1 .Fig. 4.15 Regression line FBM_2 .

The equations of the regression lines and the values of \hat{H} can be seen on Table 4.2.

Serie	Regression line	\hat{H}	H simulated
FBM1	$y = 2.74 j - 26.135$	$\hat{H}_1 = 0.87$	0.89
FBM2	$y = 2.68 j - 15.284$	$\hat{H}_2 = 0.84$	0.87

Table 4.2 Regression lines of the FBM_1 and FBM_2 (simulated data).

The equations on Table 4.2 indicate that both series contain long-memory. Additionally, the estimators have an mean square error next to zero.

Finally, we expose the coherence function between the increments according to (4.14).

For the simulated data $H_1 = 0.89$ and $H_2 = 0.87$, respectively, we get the ellipse on Fig. 4.16.

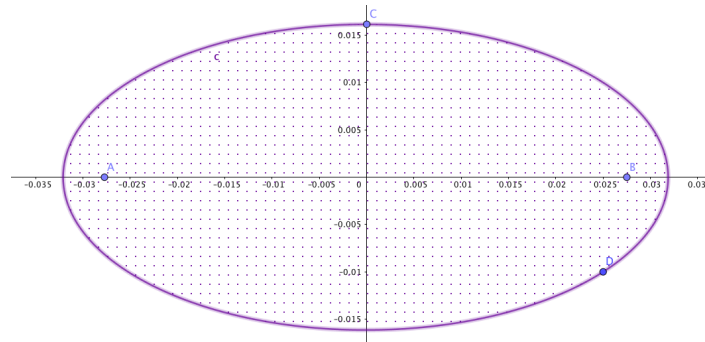


Fig. 4.16 Coherence function (ellipse on simulated data).

The equation on the ellipse is

$$\frac{\rho_{1,2}^2}{0.0011} + \frac{\eta_{1,2}^2}{0.00028} \leq 1. \quad (4.19)$$

It is important to clarify that for both cases, for the simulated data and for the real data, that the nature of the stochastic process retains a dependence relationship between the variables. For real data, the value of one currency affects the value of another; and for the simulated data, analogously.

Chapter 5

Conclusions, open questions and future works

5.1 Time copulas evolution

We have studied the violations of copula limit of time dependent family of copulas $C_t, t \geq 0$, in relation to the FX market, where violations of the Black-Scholes paradigm easily happen, often due to severe speculation. As shown in Ishimura (2014), if $C_t, t \geq 0$, satisfies heat equation then for $t \rightarrow \infty$ we obtain the Independent copula with uniform convergence. That should also accompany the convergence of Kendall's τ to zero; however, in many FX situations this convergence does not materialize (see Fig. 3.4). Also, regarding important insurance products we are specifically interested in financial/insurance products with finite time maturities. Thus, our approach, which applies Stehlik (2016) ideas financial of topological convergence of aggregation function, is a better choice for both regular and violated FX time series (see Kupka et al. (2018)).

Therefore, our work focused on the dynamic structure of the data in a way that copula parameters were not fixed, but evolved in time according to the time interval. We conclude that the theoretical version of Kendall's τ for copula C_t is given by (1.20). We have to point out that the convergence of τ time can be drastically influenced by the measure $dC(u, v)$ (see Kupka et al. (2018)).

Additionally, we observe the behavior of different groups in each of the experiments and we found the existence of different copulas when a change in the time interval is generated. Fig. 3.5 shows the evolution of parameters of copulas. For example, for the first 10 groups we get the evolution displayed in Table 3.2. Fig. 3.5 shows that there is no specific pattern

for the parameters of the copulas constructed. However, copula groups that correspond to the same family and where the parameter changes emerged.

The copulas that are obtained most often in the samples are: t-student, Tawn 2 and Frank. The Tawn copula corresponds to the family of Archimedean copulas and the t-student copula to the elliptical copula family, specifying that the latter corresponds to a copula of extreme values. In the 1000 samples extracted from the dataset, the t-student copula predominates, i.e., for some financial events the returns are not characterized by Gaussian distribution. The non-Gaussian of the returns leads to the impossibility of using Markowitz's theory for the construction of a portfolio, not to mention, the limitations in the application of some theorems for the construction of statistical models.

5.2 Assessment of long memory estimation in non-Gaussian process using copulas

We can conclude that in finance the returns of some time series do not always keep a Gaussian distribution. Repeatedly we can find returns that follow distributions of heavy tails, namely, the t-student; e.g., the frequency for the returns of CHFJPY and EUROJPY currencies of the Japanese Bank, together with the normality tests for each of the series, provide evidence that the returns do not follow a Gaussian distribution (see Fig. 4.2 and Fig. 4.3). Additionally, the bivariate stochastic process that involves both currencies through the 2-dimensional copula illustrates the bivariate t-student copula as shown in Fig. 4.4 and Fig. 4.5. Therefore, we can conclude that some time series bivariate of the FX market have a heavy tails behavior.

We also found that it is possible to establish the link between a Gaussian and non-Gaussian process using copula functions and the expression discussed in Section 4.1. Calculating the dependence coefficients in tails and constructing the 2-dimensional copula allowed us to analyze the convergence in the degrees of freedom of the bivariate process. That is, the copula functions become a useful tool for the estimation of parameters associated with the trajectories of a stochastic process.

In addition, we conclude that the use of transformation theorems on random variables, specifically the transformation of a random t-student variable in a Gaussian is possible using the inverse Gamma distribution, which is obtained using the degrees of freedom of the random t-student variable.

We also conclude that the memory of the bivariate stochastic process becomes visible through the H in each of its trajectories. That is, from the multivariate Gaussian distribution, we obtained the univariate marginals and later the value of H in each trajectory.

Therefore, we highlight that the FX market series presents volatile and erratic behavior, and the description of the probabilistic model associated with them is complex and has its own characteristics in correspondence with the nature of the data. So the TCLM model becomes an alternative for the construction and analysis of the probabilistic models in the FX market.

Finally, we can conclude the prevalence of copulas of extreme values in the FX market. However, the time range analyzed determines the nature of the subjacent copula and the implicit stochastic process. Therefore, temporal variations become a determining factor in the analysis of a stochastic process.

5.3 Open questions and future works

The possibility to study the behavior of n -dimensional financial time series remains open. That is, it would be important to set up multivariate copulas that reflect the dependence structure among several currencies.

Moreover, it would be relevant to study FX market time series that reflect a behavior of extreme values different from that of the t -student; and at the same time, it would be important to analyze the implicit memory of these processes.

It is fundamental to emphasize that in the H estimation process we must be careful. First, we must verify the assumptions associated with time series, and second, we must implement an appropriate technique. In this sense, the possibility of applying other techniques for the estimation of H , different from the DWT, remains open. Also, the possibility of comparing H estimates using other methodologies needs more attention.

Another relevant aspect would be the implementation of the TCLM model in other financial contexts, e.g., in financial series of the US FX market, i.e., studying the possibility of extrapolating the proposed method to other financial markets.

The TCLM model becomes a supporting tool for the description of the probabilistic model associated with financial series of the FX market, and therefore it would be interesting to use it for constructing investment portfolios or prediction models. Additionally, it would be important to evaluate their performance and the efficiency of the obtained estimators.

Finally, the possibility of analyzing probabilistic behavior in the evolution of the parameters associated with the constructed copulas warrants consideration. That is, the possibility of building some technique or model that evidences the subjacent variation in the dynamic evolution of the parameters, specifically in dynamic temporal windows.

References

- Abry, P., Flandrin, P., Taqqu, M., and Veitch, D. (2000). Self-similarity and long-range dependence through the wavelet lens. *Theory and applications of long-range dependence*, pages 1–25.
- Allamehzadeh, M., Kavei, M., and Mostafazadeh, M. (2015). Application of copula theory to develop techniques for earthquakes forecasting. *Journal of Seismology and Earthquake Engineering*, 17(2):81–88.
- Amblard, P.-O., Coeurjolly, J.-F., Lavancier, F., and Philippe, A. (2010). Basic properties of the multivariate fractional brownian motion. *arXiv preprint arXiv:1007.0828*.
- Bahamonde, C. (2014). *Comparación de metodologías para estimar el parámetro de Hurst en un modelo con larga Memoria*. Pontificia Universidad Católica de Valparaíso, Valparaíso.
- Beran, J., Feng, Y., Ghosh, S., and Kulik, R. (2013). *Statistics for long-memory processes. Probabilistic Properties and Statistical Methods*. Springer-Verlag Berlin Heidelberg 2013.
- Black, F. and Scholes, M. (1973). The pricing of options and corporate liabilities. *Journal of political economy*, 81(3):637–654.
- Brockwell, P. J. and Davis, R. A. (1991). Springer series in statistics.
- Cherubini, U., Gobbi, F., Mulinacci, S., and Romagnoli, S. (2013). *Dynamic, Copula Methods in Finance*. John Wiley & Sons.
- Cintas, R. (2006). Teoría de cópulas y control de riesgo financiero.
- De Mello Junior, H. D., Marti, L., da Cruz, A. V. A., and Vellasco, M. M. R. (2016). Evolutionary algorithms and elliptical copulas applied to continuous optimization problems. *Information Sciences*, 369:419–440.
- Demarta, S. and J. McNeil, A. (2004). The t copula and related copulas. *Federal Institute of Technology ETH Zentrum*.
- Erdely, A. (2017). Vectores aleatorios y sus transformaciones. *Universidad Nacional Autónoma de México*.
- Escarela, G. and Hernández, A. (2009). Modelado de parejas aleatorias usando cópulas. *Revista Colombiana de Estadística*, 32(1):33–58.
- Genest, C., Kojadinovic, I., Nešlehová, J., Yan, J., et al. (2011). A goodness-of-fit test for bivariate extreme-value copulas. *Bernoulli*, 17(1):253–275.

- Granger, C. W. and Joyeux, R. (1980). An introduction to long-memory time series models and fractional differencing. *Journal of time series analysis*, 1(1):15–29.
- Ishimura, N. (2014). Evolution of copulas and its applications. *Proceedings of the Actuarial and Financial*, page 85.
- Ishimura, N. and Yoshizawa's, Y. (2011). On time dependent bivariate copulas. 59:303–307.
- Joe, H. (1997). *Multivariate models and multivariate dependence concepts*. Chapman and Hall/CRC.
- Jones, C. L., Loneragan, G. T., and Mainwaring, D. (1996). Wavelet packet computation of the hurst exponent. *Journal of Physics A: Mathematical and general*, 29(10):2509.
- Kamal, J. B. and Haque, A. E. (2016). Dependence between stock market and foreign exchange market in South Asia: A Copula-Garch approach. *The Journal of Developing Areas*, 50(1):175–195.
- Kaplan, I. (2013). *Estimating the hurst exponent*. Independent Software Consultant and Founder, Dutch Caribbean.
- Kirichenko, L., Radivilova, T., and Deineko, Z. (2011). Comparative analysis for estimating of the hurst exponent for stationary and nonstationary time series. *Information Technologies & Knowledge*, 5(1):371–388.
- Klement, E. P., Mesiar, R., Pap, E., et al. (2001). Uniform approximation of associative copulas by strict and non-strict copulas. *Illinois Journal of Mathematics*, 45(4):1393–1400.
- Kupka, I. (2008). A topological analogue of the lipschitz condition. In *Topology proceedings*, volume 32, pages 75–81.
- Kupka, I., Kisel'ák, J., Ishimura, N., Yoshizawa, Y., Salazar, L., and Stehlík, M. (2018). Time evolutions of copulas and foreign exchange markets. *Information Sciences*, 467:163–178.
- Lavancier, F., Philippe, A., and Surgailis, D. (2009). Covariance function of vector self-similar processes. *Statistics & probability letters*, 79(23):2415–2421.
- Liu, C.-S., Chang, M.-S., Wu, X., and Chui, C. M. (2016). Hedges or safe havens—revisit the role of gold and usd against stock: a multivariate extended skew-t copula approach. *Quantitative Finance*, 16(11):1763–1789.
- Manner, H. (2007). Estimation and model selection of copulas with an application to exchange rates. *Universiteit Maastricht. Faculty of Economics and Business Administration*.
- Maya, C. and Gómez, K. (2008). What exactly is 'bad news' in foreign exchange markets?: Evidence from latin american markets. *Cuadernos de economía*, 45(132):161–183.
- Mendes, B. V., de Melo, E. F., and Nelsen, R. B. (2007). Robust fits for copula models. *Communications in Statistics—Simulation and Computation*®, 36(5):997–1017.
- Mikosch, T. (1999). Elementary stochastic calculus with finance in view.
- Nelsen, R. (2006). An Introduction to Copulas. *Springer Series in Statistics*.

- Qian, B. and Rasheed, K. (2004). Hurst exponent and financial market predictability. In *Proceedings of The 2nd IASTED international conference on financial engineering and applications*, pages 203–209.
- Quintero, F. O. L., Contreras-Reyes, J. E., and Wiff, R. (2017). Incorporating uncertainty into a length-based estimator of natural mortality in fish populations. *Fishery Bulletin*, 115(3).
- R Core, T. (2014). R: A language and environment for statistical computing. vienna, austria: R foundation for statistical computing; 2014.
- Richter, W.-D., Štěpánek, L., Ahmadinezhad, H., and Stehlík, M. (2017). Geometric aspects of robust testing for normality and sphericity. *Stochastic Analysis and Applications*, 35(3):511–532.
- Sánchez, M. Á. (2015). Estimación de parámetros y pronósticos en modelos tar con errores t-student.
- Scarsini, M. (1989). Copulae of probability measures on product spaces. *Journal of Multivariate Analysis*, 31(2):201–219.
- Shevchenko, G. (2014). Fractional brownian motion in a nutshell.
- Sklar, A. (1959). Fonctions de répartition à n dimensions et leurs marges. *Publ. Inst. Stat. Univ. Paris*, 8(8):229–231.
- Stehlik, M. (2016). On convergence of topological aggregation functions. *Fuzzy Sets and Systems*, 287:48–56.
- Villa, J. (1998). Movimiento browniano fraccionario. *Morfismos*, 2(1):47–65.
- Wei, Z. and Kim, D. (2018). On multivariate asymmetric dependence using multivariate skew-normal copula-based regression. *International Journal of Approximate Reasoning*, 92:376–391.
- Zhang, R., Czado, C., and Min, A. (2011). Efficient maximum likelihood estimation of copula based meta t-distributions. *Computational Statistics & Data Analysis*, 55(3):1196–1214.

Appendix A

Chapter I

The theorems and definitions are presented inside the Chapter 1.

Proof of Theorem 1. Proof a (see Erdely (2017)).

Let the events: $A_x := \omega \in \Omega : X(\omega) \leq x \in \mathcal{F}$ and $B_y := \omega \in \Omega : Y(\omega) \leq y \in \mathcal{F}$, such that $H_{X,Y}(x, y) = \mathbb{P}(A_x \cap B_y)$, with $y \in \mathbb{R}$ and $n \in \mathbb{N}$.

We note that $\lim_{y \rightarrow -\infty} B_y = \lim_{n \rightarrow \infty} B_{-n} = \emptyset$,

and therefore $\lim_{y \rightarrow -\infty} A_x \cap B_y = \lim_{n \rightarrow \infty} A_x \cap B_{-n} = A_x \cap \emptyset = \emptyset$.

We apply the continuity of the probability measures and obtain:

$$\begin{aligned} H_{X,Y}(x, -\infty) &= \lim_{y \rightarrow -\infty} \mathbb{P}(A_x \cap B_y) = \lim_{n \rightarrow \infty} \mathbb{P}(A_x \cap B_{-n}) = \\ \mathbb{P}(\lim_{n \rightarrow \infty} (A_x \cap B_{-n})) &= \mathbb{P}(\emptyset) = 0. \end{aligned}$$

□

Proof of Theorem 1. Proof b (see Erdely (2017)).

In this case: $\lim_{y \rightarrow +\infty} B_y = \lim_{n \rightarrow \infty} B_n = \Omega$,

and hence $\lim_{y \rightarrow +\infty} (A_x \cap B_y) = \lim_{n \rightarrow +\infty} (A_x \cap B_n) = A_x \cap \Omega = A_x$.

We apply the continuity of the probability measures and we obtain:

$$\begin{aligned} H_{X,Y}(x, +\infty) &= \lim_{y \rightarrow +\infty} \mathbb{P}(A_x \cap B_y) = \lim_{n \rightarrow \infty} \mathbb{P}(A_x \cap B_n) = \\ \mathbb{P}(\lim_{n \rightarrow \infty} (A_x \cap B_n)) &= \mathbb{P}(A_x) = F_X(x). \end{aligned}$$

□

Proof of Theorem 1. Proof c (see Erdely (2017)).

$$\begin{aligned} H_{X,Y}(+\infty, +\infty) &= \lim_{x \rightarrow +\infty} \lim_{y \rightarrow +\infty} \mathbb{P}(A_x \cap B_y) = \\ \lim_{x \rightarrow +\infty} \lim_{n \rightarrow \infty} \mathbb{P}(A_x \cap B_n) &= \lim_{x \rightarrow +\infty} \mathbb{P}(\lim_{n \rightarrow \infty} (A_x \cap B_n)) = \\ \lim_{x \rightarrow +\infty} \mathbb{P}(A_x) &= \lim_{x \rightarrow +\infty} F_X(x) = 1. \end{aligned}$$

□

Proof of Theorem 1. Proof d (see Erdely (2017)).

Let be a borelian set $D(x, y) :=]-\infty, x] \times]-\infty, y]$

such that $H_{X,Y}(x, y) = \mathbb{P}((X, Y) \in D(x, y))$.

The set $B :=]x_1, x_2] \times]y_1, y_2]$ is a borelian set in \mathbb{R}^2 such that

$$\begin{aligned} B &= (D(x_2, y_2) \setminus D(x_2, y_1)) \setminus (]-\infty, x_1] \times]y_1, y_2]), \\ B &= (D(x_2, y_2) \setminus D(x_2, y_1)) \setminus (]-\infty, x_1] \times (]-\infty, y_2] \setminus]-\infty, y_1])), \\ B &= (D(x_2, y_2) \setminus D(x_2, y_1)) \setminus (D(x_1, y_2) \setminus D(x_1, y_1)), \end{aligned}$$

and therefore,

$$\begin{aligned} 0 &\leq \mathbb{P}((X, Y) \in B) = \mathbb{P}((X, Y) \in D(x_2, y_2) \setminus D(x_2, y_1)) - \mathbb{P}((X, Y) \in D(x_1, y_2) \setminus D(x_1, y_1)) \\ &= \mathbb{P}((X, Y) \in D(x_2, y_2)) - \mathbb{P}((X, Y) \in D(x_2, y_1)) - \mathbb{P}((X, Y) \in D(x_1, y_2)) + \mathbb{P}((X, Y) \in D(x_1, y_1)), \\ 0 &\leq \mathbb{P}((X, Y) \in B) = H_{X,Y}(x_2, y_2) - H_{X,Y}(x_2, y_1) - H_{X,Y}(x_1, y_2) + H_{X,Y}(x_1, y_1). \quad \square \end{aligned}$$

Proof of Theorem 1. Proof e (see Erdely (2017)).

If $y_1 \leq y_2$, then $D(x, y_1) \subset D(x, y_2)$, thus

$$\begin{aligned} H_{X,Y}(x, y_2) - H_{X,Y}(x, y_1) &= \mathbb{P}((X, Y) \in D(x, y_2)) - \mathbb{P}((X, Y) \in D(x, y_1)), \\ H_{X,Y}(x, y_2) - H_{X,Y}(x, y_1) &= \mathbb{P}((X, Y) \in D(x, y_2) \setminus D(x, y_1)) \geq 0. \quad \square \end{aligned}$$

Proof of Theorem 1. Proof f (see Erdely (2017)).

Applying the continuity property of the probability measures:

$$\begin{aligned} \lim_{h \rightarrow 0^+} H_{X,Y}(x, y+h) &= \lim_{n \rightarrow \infty} H_{X,Y}(x, y + \frac{1}{n}), \\ \lim_{h \rightarrow 0^+} H_{X,Y}(x, y+h) &= \lim_{n \rightarrow \infty} \mathbb{P}(A_x \cap B_y + \frac{1}{n}), \\ \lim_{h \rightarrow 0^+} H_{X,Y}(x, y+h) &= \mathbb{P}(\lim_{n \rightarrow \infty} A_x \cap B_y + \frac{1}{n}), \\ \lim_{h \rightarrow 0^+} H_{X,Y}(x, y+h) &= \mathbb{P}(A_x \cap B_y) = H_{X,Y}(x, y). \quad \square \end{aligned}$$

Next, are some properties according to the definitions.

Definition 1.2

Let a function $C_{XY} : [0, 1]^2 \rightarrow [0, 1]$ and Sklar theorem: $H_{XY}(x, y) = C_{XY}(F_X(x), G_Y(y))$.

Let $u = F_X(x)$, $v = G_Y(y)$ and $C_{XY}(F_X(x), G_Y(y)) = C_{XY}(u, v)$,

$$C_{XY}(u, v) = H_{XY}(F_X^{-1}(u), G_Y^{-1}(v)), H_{XY}(x, +\infty) = F_X(x),$$

$$F_X(x) = H_{XY}(x, +\infty) = C_{XY}(F_X(x), G_Y(+\infty)), G_Y(+\infty) = 1,$$

$$F_X(x) = H_{XY}(x, +\infty) = C_{XY}(F_X(x), 1), C_{XY}(F_X(x), 1) = C_{XY}(u, 1) = u.$$

$$H_{XY}(x, -\infty) = \mathbb{P}(X \leq x, Y \leq -\infty) = 0, H_{XY}(x, -\infty) = C_{XY}(F_X(x), G_Y(-\infty)) = 0$$

$$G_Y(-\infty) = 0, H_{XY}(x, -\infty) = C_{XY}(F_X(x), 0) = 0$$

$$C_{XY}(F_X(x), 0) = C_{XY}(u, 0) = 0, 0 \leq \mathbb{P}\{(X, Y) \in]x_1, x_2] \times]y_1, y_2]\}$$

$$= H_{X,Y}(x_2, y_2) - H_{X,Y}(x_2, y_1) - H_{X,Y}(x_1, y_2) + H_{X,Y}(x_1, y_1).$$

$$\text{Sklar theorem } 0 \leq C_{XY}(u_2, v_2) - C_{XY}(u_2, v_1) - C_{XY}(u_1, v_2) + C_{XY}(u_1, v_1).$$

Definition 1.5

Remember $u = F(x)$ and $v = G(y)$,

Then $x = F^{-1}(u)$ and $y = G^{-1}(v)$

Then $X = F^{-1}(U)$ and $Y = G^{-1}(V)$

We apply theorem of linear transformations of continuous random variables

$c(u, v) = h(F^{-1}(u), G^{-1}(v)) \times A$

with

$$A = \begin{vmatrix} \frac{\partial x}{\partial u} & \frac{\partial x}{\partial v} \\ \frac{\partial y}{\partial u} & \frac{\partial y}{\partial v} \end{vmatrix}$$

$x = F^{-1}(u)$, then $\frac{\partial x}{\partial u} = \frac{\partial F^{-1}(u)}{\partial u}$

Propertie: $(f^{-1})'(a) = \frac{1}{f'(f^{-1}(a))}$,

in our case: $(F^{-1})'(u) = \frac{1}{f(F^{-1}(u))}$,

$$\frac{\partial F^{-1}(u)}{\partial u} = \frac{1}{f(F^{-1}(u))}$$

$$\frac{\partial F^{-1}(u)}{\partial v} = 0$$

$$\frac{\partial G^{-1}(V)}{\partial v} = \frac{1}{g(G^{-1}(V))}$$

$$\frac{\partial G^{-1}(V)}{\partial u} = 0$$

$$A = \begin{vmatrix} \frac{\partial X}{\partial u} & \frac{\partial X}{\partial v} \\ \frac{\partial Y}{\partial u} & \frac{\partial Y}{\partial v} \end{vmatrix} = \left(\frac{\partial X}{\partial u} \times \frac{\partial Y}{\partial v} \right) - \left(\frac{\partial X}{\partial v} \times \frac{\partial Y}{\partial u} \right),$$

$$\left(\frac{\partial X}{\partial u} \times \frac{\partial Y}{\partial v} \right) - \left(\frac{\partial X}{\partial v} \times \frac{\partial Y}{\partial u} \right) = \left(\frac{\partial F^{-1}(U)}{\partial u} \times \frac{\partial G^{-1}(V)}{\partial v} \right) - \left(\frac{\partial F^{-1}(U)}{\partial v} \times \frac{\partial G^{-1}(V)}{\partial u} \right),$$

$$\left(\frac{\partial F^{-1}(U)}{\partial u} \times \frac{\partial G^{-1}(V)}{\partial v} \right) - \left(\frac{\partial F^{-1}(U)}{\partial v} \times \frac{\partial G^{-1}(V)}{\partial u} \right) = \left(\frac{1}{f(F^{-1}(U))} \times \frac{1}{g(G^{-1}(V))} \right) - 0,$$

$$\left(\frac{\partial F^{-1}(U)}{\partial u} \times \frac{\partial G^{-1}(V)}{\partial v} \right) - \left(\frac{\partial F^{-1}(U)}{\partial v} \times \frac{\partial G^{-1}(V)}{\partial u} \right) = \frac{1}{(f(F^{-1}(U)) \times g(G^{-1}(V)))} = \frac{1}{f(x)g(y)},$$

then $A = \frac{1}{f(x)g(y)}$,

Replacing in $c(u, v) = h(F^{-1}(u), G^{-1}(v)) \times A$,

we obtain $c(u, v) = \frac{h(x, y)}{f(x)g(y)}$.

Proof of Theorem 4.

From the triangle inequality, we have

$$|H(x_2, y_2) - H(x_1, y_1)| \leq |H(x_2, y_2) - H(x_1, y_2)| + |H(x_1, y_2) - H(x_1, y_1)|.$$

Now assume $x_1 \leq x_2$.

Because H is grounded, 2-increasing and exhibit the marginals

yield $0 \leq H(x_2, y_2) - H(x_1, y_2) \leq F(x_2) - F(x_1)$.

An analogous inequality holds when $x_2 \leq x_1$, hence it follows that for any x_1, x_2 in S_1 ,

$$|H(x_2, y_2) - H(x_1, y_2)| \leq |F(x_2) - F(x_1)|.$$

$$\text{Similarly for any } y_1, y_2 \text{ in } S_2, |H(x_1, y_2) - H(x_1, y_1)| \leq |G(y_2) - G(y_1)|.$$

Replacing

$$|H(x_2, y_2) - H(x_1, y_2)| \leq |F(x_2) - F(x_1)| \text{ and } |H(x_1, y_2) - H(x_1, y_1)| \leq |G(y_2) - G(y_1)|$$

$$\text{in } |H(x_2, y_2) - H(x_1, y_1)| \leq |H(x_2, y_2) - H(x_1, y_2)| + |H(x_1, y_2) - H(x_1, y_1)|,$$

We obtain,

$$|H(x_2, y_2) - H(x_1, y_1)| \leq |F(x_2) - F(x_1)| + |G(y_2) - G(y_1)|.$$

□

Definition 1.6

Let (u, v) be an arbitrary point in $DomC$

$$\text{Now, } C(u, v) \leq C(u, 1) = u \text{ and } C(u, v) \leq C(1, v) = v$$

$$\text{yield } C(u, v) \leq \min(u, v).$$

$$\text{Furthermore, } V_C([u, 1] \times [v, 1]) \geq 0$$

$$\text{implies } V_C([u, 1] \times [v, 1]) = C(1, 1) - C(1, v) - C(u, 1) + C(u, v) \geq 0,$$

$$C(1, 1) - C(1, v) - C(u, 1) + C(u, v) = 1 - v - u + C(u, v) \geq 0,$$

$$C(u, v) \geq u + v - 1,$$

$$\text{which when combined with } C(u, v) \geq 0,$$

$$\text{yields } C(u, v) \geq \max(u + v - 1, 0).$$

Proof of Theorem 7.

$$Q = P[(X_1 - X_2)(Y_1 - Y_2) > 0] - P[(X_1 - X_2)(Y_1 - Y_2) < 0]$$

$$P[(X_1 - X_2)(Y_1 - Y_2) < 0] = 1 - P[(X_1 - X_2)(Y_1 - Y_2) > 0],$$

$$Q = 2P[(X_1 - X_2)(Y_1 - Y_2) > 0] - 1$$

$$P[(X_1 - X_2)(Y_1 - Y_2) > 0] = P[(X_1 > X_2, Y_1 > Y_2)] + P[(X_1 < X_2, Y_1 < Y_2)]$$

$$P[(X_1 > X_2, Y_1 > Y_2)] = P[(X_2 < X_1, Y_2 < Y_1)],$$

$$\text{Remember, } H_{XY}(x, y) = P(X \leq x, Y \leq y),$$

$$H_{XY}(x, y) = C(F_X(x), G_Y(y)),$$

$$P[(X_2 < X_1, Y_2 < Y_1)] = H_{X_2Y_2}(X_1, Y_1)$$

$$H_{X_2Y_2}(X_1, Y_1) = C(F_{X_2}(X_1), G_{Y_2}(Y_1)),$$

$$C(F_{X_2}(X_1), G_{Y_2}(Y_1)) = C_2(F_X(X_1), G_Y(Y_1)),$$

$$\text{Remember, } H_{X_2Y_2}(X_1, Y_1) = P[(X_2 < X_1, Y_2 < Y_1)] = \int_{-\infty}^{X_1} \int_{-\infty}^{Y_1} h(s, t) ds dt,$$

$$ds = \frac{\partial}{\partial X_1} H_{X_2Y_2}(X_1, Y_1),$$

$$\frac{\partial}{\partial X_1} H_{X_2Y_2}(X_1, Y_1) = \frac{\partial}{\partial X_1} C_2(F_X(X_1), G_Y(Y_1)),$$

$$P[(X_2 < X_1, Y_2 < Y_1)] = \int \int_{\mathbb{R}^2} P[(X_2 < x, Y_2 < y)] dC_1(F(x), G(y)),$$

$$P[(X_2 < x, Y_2 < y)] = C_2(F_X(x), G_Y(y)),$$

$$P[(X_2 < X_1, Y_2 < Y_1)] = \int \int_{\mathbb{R}^2} C_2(F_X(x), G_Y(y)) dC_1(F(x), G(y)),$$

$$P[(X_2 < X_1, Y_2 < Y_1)] = \int \int_{\mathbf{I}^2} C_2(u, v) dC_1(u, v).$$

Remember, $\bar{H}(x, y) = 1 - F(x) - G(y) + H(x, y)$

$$\bar{H}(x, y) = P[(X > x, Y > y)]$$

Now, $P[(X_2 > X_1, Y_2 > Y_1)] = \bar{H}_{X_2 Y_2}(X_1, Y_1)$

$$\bar{H}_{X_2 Y_2}(X_1, Y_1) = 1 - F_{X_2}(X_1) - G_{Y_2}(Y_1) + H_{X_2 Y_2}(X_1, Y_1)$$

$$\bar{H}_{X_2 Y_2}(X_1, Y_1) = 1 - F_{X_2}(X_1) - G_{Y_2}(Y_1) + C_2(F_X(X_1), G_Y(Y_1))$$

$$P[(X_2 > X_1, Y_2 > Y_1)] = \int \int_{\mathbb{R}^2} P[(X_2 > x, Y_2 > y)] dC_1(F(x), G(y))$$

$$P[(X_2 > X_1, Y_2 > Y_1)] = \int \int_{\mathbb{R}^2} [1 - F(x) - G(y) + C_2(F(x), G(y))] dC_1(F(x), G(y))$$

$$P[(X_2 > X_1, Y_2 > Y_1)] = \int \int_{\mathbf{I}^2} [1 - u - v + C_2(u, v)] dC_1(u, v)$$

$$\int \int_{\mathbf{I}^2} dC_1(u, v) = \int_0^1 \int_0^1 dC_1(u, v)$$

$$\int_0^1 \int_0^1 dC_1(u, v) = \int_0^1 C_1(u, v) \Big|_0^1 dv \text{ en } u$$

$$\int_0^1 \int_0^1 dC_1(u, v) = \int_0^1 (C_1(1, v) - C_1(0, v)) dv$$

$$\int_0^1 \int_0^1 dC_1(u, v) = \int_0^1 (1 - 0) dv$$

$$\int_0^1 \int_0^1 dC_1(u, v) = \int_0^1 dv$$

$$\int_0^1 \int_0^1 dC_1(u, v) = v \Big|_0^1 = 1$$

$$\int \int_{\mathbf{I}^2} u dC_1(u, v) = \int_0^1 \int_0^1 u dC_1(u, v)$$

$$\int_0^1 \int_0^1 u dC_1(u, v) = \int_0^1 \left[\frac{u^2}{2} \right]_0^1 dv \text{ in } u$$

$$\int_0^1 \int_0^1 u dC_1(u, v) = \int_0^1 \left(\frac{1}{2} - \frac{0}{2} \right) dv$$

$$\int_0^1 \int_0^1 u dC_1(u, v) = \frac{1}{2} \int_0^1 dv = \frac{1}{2}$$

$$P[(X_2 > X_1, Y_2 > Y_1)] = \int \int_{\mathbf{I}^2} [1 - u - v + C_2(u, v)] dC_1(u, v)$$

$$P[(X_2 > X_1, Y_2 > Y_1)] = 1 - \frac{1}{2} - \frac{1}{2} + \int \int_{\mathbf{I}^2} [C_2(u, v)] dC_1(u, v)$$

$$P[(X_2 > X_1, Y_2 > Y_1)] = \int \int_{\mathbf{I}^2} [C_2(u, v)] dC_1(u, v)$$

Substituting in $P[(X_1 - X_2)(Y_1 - Y_2) > 0] =$

$$P[(X_1 > X_2, Y_1 > Y_2)] + P[(X_1 < X_2, Y_1 < Y_2)]$$

$$\begin{aligned}
P[(X_1 - X_2)(Y_1 - Y_2) > 0] &= \int \int_{\mathbf{I}^2} [C_2(u, v)] dC_1(u, v) + \int \int_{\mathbf{I}^2} [C_2(u, v)] dC_1(u, v) \\
P[(X_1 - X_2)(Y_1 - Y_2) > 0] &= 2 \int \int_{\mathbf{I}^2} [C_2(u, v)] dC_1(u, v) \\
Q &= 2P[(X_1 - X_2)(Y_1 - Y_2) > 0] - 1 \\
Q &= 2 \left(2 \int \int_{\mathbf{I}^2} [C_2(u, v)] dC_1(u, v) \right) - 1 \\
Q &= 4 \int \int_{\mathbf{I}^2} [C_2(u, v)] dC_1(u, v) - 1.
\end{aligned}$$

□

Definition 1.15

$$\bar{H}(x, y) = 1 - F(x) - G(y) + H(x, y)$$

$$\bar{H}(x, y) = \bar{F}(x) + \bar{G}(y) - 1 + C(F(x), G(y))$$

$$\bar{F}(x) = 1 - F(x) \text{ and } \bar{G}(y) = 1 - G(y)$$

$$\bar{H}(x, y) = \bar{F}(x) + \bar{G}(y) - 1 + C(1 - \bar{F}(x), 1 - \bar{G}(y))$$

$$\text{If } u = \bar{F}(x) \text{ and } v = \bar{G}(y)$$

$$\bar{H}(x, y) = u + v - 1 + C(1 - u, 1 - v)$$

$$\text{We define } \bar{H}(x, y) = \hat{C}(\bar{F}(x), \bar{G}(y)) = \hat{C}(u, v)$$

$$\hat{C}(u, v) = u + v - 1 + C(1 - u, 1 - v)$$

$$\hat{C}(1 - u, 1 - v) = 1 - u + 1 - v - 1 + C(1 - (1 - u), 1 - (1 - v))$$

$$\hat{C}(1 - u, 1 - v) = 1 - u - v + C(u, v) = \bar{C}(u, v).$$

Proof of Theorem 12.

$$\text{Boundary conditions: } C(u, 0) = \varphi^{[-1]}(\varphi(u) + \varphi(0)) = 0$$

$$C(0, v) = \varphi^{[-1]}(\varphi(0) + \varphi(v)) = 0$$

$$C(u, 1) = \varphi^{[-1]}(\varphi(u) + \varphi(1)) = u$$

$$C(u, 1) = \varphi^{[-1]}(\varphi(u) + 0) = u$$

$$C(u, 1) = \varphi^{[-1]}(\varphi(u)) = u$$

$$C(1, v) = \varphi^{[-1]}(\varphi(1) + \varphi(v)) = v$$

$$C(1, v) = \varphi^{[-1]}(0 + \varphi(v)) = v$$

$$C(1, v) = \varphi^{[-1]}(\varphi(v)) = v$$

2-increasing:

We use the theorem:

Let φ , $\varphi^{[-1]}$ and C satisfy the hypotheses of Theorem 4. Then C is 2-increasing if and only if for all v in \mathbf{I} , whenever $u_1 \leq u_2$, $C(u_2, v) - C(u_1, v) \leq u_2 - u_1$.

Choose v_1, v_2 in \mathbf{I} such that $v_1 \leq v_2$, and note that

$$C(0, v_2) = 0 \leq v_1 \leq v_2 = C(1, v_2).$$

But C is continuous (because φ and $\varphi^{[-1]}$ are), and thus there is a t in \mathbf{I} such that

$$C(t, v_2) = v_1, \text{ or } \varphi(v_2) + \varphi(t) = \varphi(v_1)$$

Now $u_1 \leq u_2$ and we analyze $C(u_2, v_1) - C(u_1, v_1)$

$$C(u_2, v_1) - C(u_1, v_1) = \varphi^{[-1]}(\varphi(u_2) + \varphi(v_1)) - \varphi^{[-1]}(\varphi(u_1) + \varphi(v_1))$$

$$C(u_2, v_1) - C(u_1, v_1) = \varphi^{[-1]}(\varphi(u_2) + \varphi(v_2) + \varphi(t)) - \varphi^{[-1]}(\varphi(u_1) + \varphi(v_2) + \varphi(t))$$

$$\varphi(u_2) + \varphi(v_2) = \varphi(m)$$

$$\varphi(u_1) + \varphi(v_2) = \varphi(n)$$

$$C(u_2, v_1) - C(u_1, v_1) = \varphi^{[-1]}(\varphi(m) + \varphi(t)) - \varphi^{[-1]}(\varphi(n) + \varphi(t))$$

$$C(u_2, v_1) - C(u_1, v_1) = C(m, t) - C(n, t)$$

$$C(u_2, v_1) - C(u_1, v_1) = C(C(u_2, v_2), t) - C(C(u_1, v_2), t)$$

$$C(u_2, v_1) - C(u_1, v_1) \leq C(u_2, v_2) - C(u_1, v_2).$$

□

Proof of Theorem 16.

\implies

hypothesis: C is a max-stable copula

thesis: C is an extreme value copula

Definition, every max-stable copula is an extreme value copula.

\impliedby

hypothesis: C is an extreme value copula

thesis: C is a max-stable copula

$$C_*(u, v) = \lim_{n \rightarrow \infty} C^n(u^{\frac{1}{n}}, v^{\frac{1}{n}})$$

$$C_*^r(u^{\frac{1}{r}}, v^{\frac{1}{r}}) = \lim_{n \rightarrow \infty} C^{rn}(u^{\frac{1}{rn}}, v^{\frac{1}{rn}}) = C_*(u, v)$$

$$C_*^r(u^{\frac{1}{r}}, v^{\frac{1}{r}}) = C_*(u, v), C \text{ is max-stable.}$$

□

Appendix B

Chapter III

All the setting-up and estimates have been carried out using of the R software (R Core (2014)). Here we present the code for the construction of copula functions and the different measures. In this chapter, we use the packages: copula, VineCopula, MASS, rgl, readr, fCopulae, ggplot2, dplyr, PerformanceAnalytics, urca, MASS, tseries, scales, psych and PerformanceAnalytics.

Libraries

```
library("copula")
library("VineCopula")
library("MASS")
library("rgl")
library("readr")
library("fCopulae")
library("ggplot2")
library("dplyr")
library("PerformanceAnalytics")
library("urca")
library("MASS")
library("tseries")
library("scales")
library("psych")
library("PerformanceAnalytics")
```

Currency time series

```

date1$CHFJPY <- as.numeric( gsub(",", ".", date$CHFJPY))
date1$EUROJPY <- as.numeric( gsub(",", ".", date$EUROJPY))
j <- seq(from=1, to=1931, by=1)
e1 <- data.frame(j, (date1[,1]))
e2 <- data.frame(j, (date1[,2]))
names(e1)[1] <- 'Data'
names(e2)[1] <- 'Data'
names(e1)[2] <- 'Currency'
names(e2)[2] <- 'Currency'
e1$Exchange <- "CHFJPY"
e2$Exchange <- "EUROJPY"
data.all <- data.frame(rbind(e1, e2))
ts <- ggplot() + geom_line(data=data.all, aes(x=Data, y=Currency,
      colour = Exchange, group=Exchange), size=0.5) +theme_minimal()
      + scale_color_manual(values=c("seagreen", "olivedrab"))
print(ts)

```

Time series returns

```

listCHFJPYr <- list()
for(i in 1:1931) {
listCHFJPYr[[i]] <- (log(date1[i+1,1]) - log(date1[i,1]))
}
listCHFJPYr <- do.call(rbind, listCHFJPYr)
j <- seq(from=1, to=1930, by=1)
r1 <- data.frame(j, listCHFJPYr[1:1930,])
names(r1)[1] <- 'Data'
names(r1)[2] <- 'Return'
data.allr1 <- r1
tsCHFJPYr <- ggplot() + geom_point(data=data.allr1,
      aes(x=Data, y=Return), size=0.5, color='seagreen')
      + theme_minimal() + scale_color_manual(values=
      c("seagreen"))+ ylim(-0.03,0.03)
print(tsCHFJPYr)

```

```

listEUROJPYr <- list()
for(i in 1:1931) {
listEUROJPYr[[i]] <- (log(date1[i+1,2]) - log(date1[i,2]))
}
listEUROJPYr <- do.call(rbind, listEUROJPYr)
j <- seq(from=1, to=1930, by=1)
r2 <- data.frame(j, listEUROJPYr[1:1930,])
names(r2)[1] <- 'Data'
names(r2)[2] <- 'Return'
data.allr2 <- r2
tsEUROJPYr <- ggplot() + geom_point(data=data.allr2,
aes(x=Data, y=Return), size=0.5, color='olivedrab')
+ theme_minimal() + scale_color_manual(values=
c("olivedrab"))+ ylim(-0.03,0.03)
print(tsEUROJPYr)

```

Copula function on the samples

```

data <- cbind(listCHFJPYr, listEUROJPYr)
k <- 100
h <- 1
INT <- 1000
lista.data <- list()
lista.cop <- list()
lista.tau <- list()
lista.emptau <- list()
lista.cor <- list()
lista.cor.spearman <- list()
lista.cor.pearson <- list()
j <- 1
for(i in k:(k+INT)) {
lista.cop[[j]] <- BiCopSelect(pobs(data[(h:i),1]), pobs(data[(h:i),2]), familyset=NA)
lista.data[[j]] <- data[h:i,]
lista.tau[[j]] <- lista.cop[[j]]$tau
lista.emptau[[j]] <- lista.cop[[j]]$emptau
lista.cor[[j]] = cor(pobs(as.matrix(data[(h:i),1])), pobs(as.matrix(data[(h:i),2])),method="kendall")
lista.cor.spearman[[j]] = cor((as.matrix(data[(h:i),1])), (as.matrix(data[(h:i),2])),method="spearman")

```

```

lista.cor.pearson[[j]] = cor((as.matrix(data[(h:i),1])), (as.matrix(data[(h:i),2])),method="pearson")
j <- j + 1
h <- h + 1
}
tau <- do.call(rbind, lista.tau)
emptau <- do.call(rbind, lista.emptau)
lista <- do.call(rbind, lista.cop)
cor <- do.call(rbind, lista.cor)
cor.spearman <- do.call(rbind, lista.cor.spearman)
cor.pearson <- do.call(rbind, lista.cor.pearson)
comp <- cbind(cor, cor.spearman, tau, emptau, cor.pearson)

```

Kendall's τ on 50 copulas

```

j50 <- seq(from=1, to=50, by=1)
data50 <- data.frame(j50, emptau[1:50,1])
names(data50)[1] <- 'Data'
names(data50)[2] <- 'Kendall-tau'
data.all50 <- data.frame(data50)
tau_data.all50 <- ggplot() + geom_line(data=data.all50, aes(x=data.all50[,1],
y=data.all50[,2]), colour="#436EEE", size=1) + labs(x="Data",
y="Kendall-tau") + theme_minimal()
png(file = "f3_1_4.png", bg = "transparent", res = 600, width = 3200,
height = 2000, units = "px")
print(tau_data.all50)
dev.off()

```

Kendall's τ on 100 copulas

```

j100 <- seq(from=1, to=100, by=1)
data100 <- data.frame(j100, emptau[1:100,1])
names(data100)[1] <- 'Data'
names(data100)[2] <- 'Kendall-tau'
data.all100 <- data.frame(data100)
tau_data.all100 <- ggplot() + geom_line(data=data.all100, aes(x=data.all100[,1],
y=data.all100[,2]), colour="#436EEE", size=1) + labs(x="Data",
y="Kendall-tau") + theme_minimal()
png(file = "f3_2_4.png", bg = "transparent", res = 600, width = 3200,

```

```
    height = 2000, units = "px")
print(tau_data.all100)
dev.off()
```

Kendall's τ on 500 copulas

```
j500 <- seq(from=1, to=500, by=1)
data500 <- data.frame(j500, emptau[1:500,1])
names(data500)[1] <- 'Data'
names(data500)[2] <- 'Kendall-tau'
data.all500 <- data.frame(data500)
tau_data.all500 <- ggplot() + geom_line(data=data.all500, aes(x=data.all500[1],
    y=data.all500[2]), colour="#436EEE", size=1) + labs(x="Data",
    y="Kendall-tau") + theme_minimal()
png(file = "f3_3_4.png", bg = "transparent", res = 600, width = 3200,
    height = 2000, units = "px")
print(tau_data.all500)
dev.off()
```

Kendall's τ on 1000 copulas

```
j1000 <- seq(from=1, to=1000, by=1)
data1000 <- data.frame(j1000, emptau[1:1000,1])
names(data1000)[1] <- 'Data'
names(data1000)[2] <- 'Kendall-tau'
data.all1000 <- data.frame(data1000)
tau_data.all1000 <- ggplot() + geom_line(data=data.all1000, aes(x=data.all1000[1],
    y=data.all1000[2]), colour="#436EEE", size=1) + labs(x="Data",
    y="Kendall-tau") + theme_minimal()
png(file = "f3_4_4.png", bg = "transparent", res = 600, width = 3200,
    height = 2000, units = "px")
print(tau_data.all1000)
dev.off()
```

Par and par2 evolution on 1000 copulas

```
id <- seq(from=1, to=1001, by=1)
datag <- data.frame(cbind(id,data.frame(lista[,2:3]), t(data.frame(lista[,5]))))
names(datag)[4] <- 'Copula'
```

```

glimpse(lista)
pars <- ggplot() + geom_line(data=datag, aes(x=id, y=as.numeric(datag$par)),
  colour="gray70" )+ geom_line(data=datag, aes(x=id, y=as.numeric(datag$par2)),
  colour="gray18") + geom_point(data=datag, aes(x=id, y=as.numeric(datag$par),
  colour =Copula), size=0.5) + geom_point(data=datag, aes(x=id,
  y=as.numeric(datag$par2), colour=Copula), size=0.5)
+ xlab('Data') + ylab('Parameters') + theme_minimal()
+ theme(legend.text = element_text(colour="black", size = 10,
  face = "bold"), legend.direction = "horizontal",
  legend.position = "bottom") + theme(legend.position="bottom")
png(file = "f3_1_5.png", bg = "transparent", res = 600,width = 3200,
  height = 2000, units = "px")
print(pars)
dev.off()

```

Densities of the t-student copula for the 5 and 548 samples

```

persp(tCopula(par=0.766141949496352), dCopula, zlim = c(0,10),
col = "#9BCD9B", xlab = "u", ylab = "v", zlab = "c(u,v)", shade = 0.1)
persp(tCopula(par=0.707735419135883), dCopula, zlim = c(0,10),
col = "#CDAA7D", xlab = "u", ylab = "v", zlab = "c(u,v)", shade = 0.1)

```

Upper and lower bounds for Spearman's ρ coefficient

```

sp1 <- data.frame(((3*emptau[,1])+1)/2)
sp2 <- data.frame(((3*emptau[,1])-1)/2)
j <- seq(from=1, to=1001, by=1)
e1 <- data.frame(j, cor.spearman[,1])
e4 <- data.frame(j, sp1)
e5 <- data.frame(j, sp2)
names(e1)[1] <- 'Data'
names(e4)[1] <- 'Data'
names(e5)[1] <- 'Data'
names(e1)[2] <- 'Bounds'
names(e4)[2] <- 'Bounds'
names(e5)[2] <- 'Bounds'
e1$Coef <- "Spearman-rho"
e4$Coef <- "Spearman upper"

```

```
e5$Coef <- "Spearman lower"
data.all <- data.frame(rbind(e1, e4, e5))
tsblus <- ggplot() + geom_line(data=data.all, aes(x=Data, y=Bounds,
          colour = Coef, group=Coef), size=0.5) + theme_minimal() +
          scale_color_manual(values=c("#CD2990", "#CD2990", "#8B4789" )) +
          ylim(-0.5,2)
print(tsblus)
```

Upper and lower bounds for Kendall's *tau* coefficient

```
t1 <- data.frame(((2*cor.spearman[,1])+1)/3)
t2 <- data.frame(((2*cor.spearman[,1])-1)/3)
j <- seq(from=1, to=1001, by=1)
e1 <- data.frame(j, emptau[,1])
e4 <- data.frame(j, t1)
e5 <- data.frame(j, t2)
names(e1)[1] <- 'Data'
names(e4)[1] <- 'Data'
names(e5)[1] <- 'Data'
names(e1)[2] <- 'Bounds'
names(e4)[2] <- 'Bounds'
names(e5)[2] <- 'Bounds'
e1$Coef <- "Kendall-tau"
e4$Coef <- "Kendall upper"
e5$Coef <- "Kendall lower"
data.all <- data.frame(rbind(e1, e4, e5))
tsblut <- ggplot() + geom_line(data=data.all, aes(x=Data, y=Bounds,
          colour = Coef, group=Coef), size=0.5) + theme_minimal() +
          scale_color_manual(values=c("#66CDAA", "#66CDAA", "#436EEE")) +
          ylim(-0.5,2)
print(tsblut)
```


Appendix C

Chapter IV

All the setting-up and estimates have been carried out using of the R software. Here we present the code. In this chapter we use the packages: copula, VineCopula, MASS, rgl, readr, fCopulae, ggplot2, dplyr, PerformanceAnalytics, urca, MASS, tseries, scales, psych and PerformanceAnalytics.

Libraries

```
library("copula")
library("MASS")
library("psych")
library("rgl")
library("VineCopula")
library("reader")
library("PerformanceAnalytics")
library("wavelets")
library("ggplot2")
library("mvtnorm")
library("scatterplot3d")
library("plot3D")
library("hypergeo")
```

Histogram of the CHFJPY time series

```
listCHFJPYr <- list()
for(i in 1:1931) { listCHFJPYr[[i]] <- (log(date1[i+1,1]) - log(date1[i,1]))
}
listCHFJPYr <- do.call(rbind, listCHFJPYr)
```

```

r <- listCHFJPYr
j <- seq(from=1, to=1930, by=1)
h1 <- data.frame(j, r[1:1930,1])
names(h1)[1] <- 'Dato'
names(h1)[2] <- 'Retorno'
data.allh1 <- h1
histpar1 <- ggplot(data=data.allh1, aes(as.numeric(data.allh1$Retorno))) +
  labs(x="Returns", y="Count") + theme_minimal () + geom_histogram
  (bins = 1200, colour="seagreen") + xlim(-0.044, 0.044) + ylim(0,80) +
  theme(legend.position="none")
png(file = "f4_2.png", bg = "transparent", res = 600,width = 3200,
  height = 2000, units = "px")
print(histpar1)
dev.off()
shapiro.test(r)

```

Histogram of the EUROJPY time series

```

listEUROJPYr <- list()
for(i in 1:1931) {
listEUROJPYr[[i]] <- (log(date1[i+1,2]) - log(date1[i,2]))
}
listEUROJPYr <- do.call(rbind, listEUROJPYr)
r <- listEUROJPYr
j <- seq(from=1, to=1930, by=1)
h2 <- data.frame(j, r[1:1930,1])
names(h2)[1] <- 'Dato'
names(h2)[2] <- 'Retorno'
data.allh2 <- h2
histpar2 <- ggplot(data=data.allh2, aes(as.numeric(data.allh2$Retorno))) +
  labs(x="Returns", y="Count") + theme_minimal () + geom_histogram
  (bins = 1200, colour="olivedrab") + xlim(-0.046, 0.046) + ylim(0,80)
png(file = "f4_3.png", bg = "transparent", res = 600,width = 3200,
  height = 2000, units = "px")
print(histpar2)
dev.off()

```

```
shapiro.test(r)
```

Real data

Copula on the all data set

```
dr <- cbind(listCHFJPYr, listEUROJPYr)
ctreal <- BiCopSelect(pobs(dr[,1]), pobs(dr[,2]), familyset=NA)
persp(tCopula(par=0.76), pCopula, zlim = c(0,1), col = "#698B69",
xlab = "u", ylab = "v", zlab = "C(u,v)")
dev.copy(png, 'f4_6.png')
dev.off()
persp(tCopula(par=0.76), dCopula, zlim = c(0,8), col = "#698B69",
xlab = "u", ylab = "v", zlab = "c(u,v)")
dev.copy(png, 'f4_4.png')
dev.off()
contour(tCopula(par=0.76), pCopula, zlim = c(0,1), col= "#698B69",
xlab = "u", ylab = "v", zlab = "C(u,v)", lty = "solid")
contour(tCopula(par=0.76), dCopula, zlim = c(0,1), col= "#698B69",
xlab = "u", ylab = "v", zlab = "C(u,v)", lty = "solid")
dev.copy(png, 'f4_5.png')
dev.off()
```

Equation 4.11 \hat{v} in the bivariate process

```
df<-list()
la<- 0.564
for(i in 1:(20)) {
df[[i]] <- la-(((0.940881) $\hat{v}^{i+1}$ )*f21hyper(1/2,((i+1)/2),((i+3)/2),0.885257) -
(6.12323*10 $\hat{v}^{-17}$ ))*(6.12323*10 $\hat{v}^{-17}$ *i)*f21hyper(1/2,((i+1)/2),((i+3)/2),
(3.7494*10 $\hat{v}^{-33}$ ))) $\hat{v}^2$ *gamma((i/2)+1)/(sqrt(pi)*gamma((i+1)/2)*(i+1))
}
cd <- do.call(rbind, df)
jd <- seq(from=1, to=20, by=1)
hd <- data.frame(jd, cd)
names(hd)[1] <- 'd'
names(hd)[2] <- 'f'
data.allhd <- hd
```

```

freedomhd <- ggplot(data=data.allhd, aes(x=as.numeric(data.allhd$d),
      y=as.numeric(data.allhd$f)) ) + labs(x="df ",y="df function ") +
      geom_point(colour="#43CD80") + theme_minimal()
      + xlim(0,20) + ylim(0,0.3)
png(file = "f4_7.png", bg = "transparent", res = 600,width = 3200,
      height = 2000, units = "px")
print(freedomhd)
dev.off()

```

Gamma distribution

```

gmat <- dgamma((matrix(c(1:4), nrow=2, ncol=2, byrow = TRUE)), 2, 2)
gmat <- as.matrix(gmat)
igmat <- solve(gmat)

```

Gaussian distribution

```

normv <- dr
normv <- normv[1:1930,]
n1 <- normv[1:1930,1]
n2 <- normv[1:1930,2]
n1 <- data.frame(normv[1:1930,1])
n2 <- data.frame(normv[1:1930,2])
n11 <- list()
for(i in 1:1930) {
n11[[i]]<-(n1[i+1,1] - n1[i,1])
}
n1n <- do.call(rbind, n11)
n1n <- n1n[1:1929,]
shapiro.test(n1n)
n22 <- list()
for(i in 1:1930) {
n22[[i]] <- (n2[i+1,1] - n2[i,1])
}
n2n <- do.call(rbind, n22)
n2n <- n2n[1:1929,]
shapiro.test(n2n)

```

DWT method

Regression line on FMB_1

```

n1 <- normv[1:1930,1]
dw1 <- dwt(n1, n.levels = 10, fast = FALSE)
s1 <- log2(sum((dw1@W$W1)^2)/length(dw1@W$W1))
s2 <- log2(sum((dw1@W$W2)^2)/length(dw1@W$W2))
s3 <- log2(sum((dw1@W$W3)^2)/length(dw1@W$W3))
s4 <- log2(sum((dw1@W$W4)^2)/length(dw1@W$W4))
s5 <- log2(sum((dw1@W$W5)^2)/length(dw1@W$W5))
s6 <- log2(sum((dw1@W$W6)^2)/length(dw1@W$W6))
s7 <- log2(sum((dw1@W$W7)^2)/length(dw1@W$W7))
s8 <- log2(sum((dw1@W$W8)^2)/length(dw1@W$W8))
s9 <- log2(sum((dw1@W$W9)^2)/length(dw1@W$W9))
s10 <- log2(sum((dw1@W$W10)^2)/length(dw1@W$W10))
jw <- seq(from=1, to=10, by=1)
hw <- data.frame(jw, c(s1, s2, s3, s4, s5, s6, s7, s8, s9, s10))
names(hw)[1] <- 'l'
names(hw)[2] <- 'H'
data.allhw <- hw
n1graph <- ggplot(data=data.allhw, aes(x=as.numeric(data.allhw$l),
      y=as.numeric(data.allhw$H)) ) + theme_minimal()+labs(x="level j",
      + y="H function") geom_point(colour="seagreen", size=1)
      + geom_smooth(method='lm', formula=y ~ x, colour="seagreen",
      se=FALSE) + ylim(-10,5)
png(file = "f4_8.png", bg = "transparent", res = 600,width = 3200,
      height = 2000, units = "px")
print(n1graph)
dev.off()
lm(H ~ l, data = data.allhw)

```

Regression line on FMB_2

```

n2 <- normv[1:1930,2]
dw2<- dwt(n2, n.levels = 10, fast = FALSE)
s21 <- log2(sum((dw2@W$W1)^2)/length(dw1@W$W1))
s22 <- log2(sum((dw2@W$W2)^2)/length(dw1@W$W2))

```

```

s23 <- log2(sum((dw2@W$W3)^2)/length(dw1@W$W3))
s24 <- log2(sum((dw2@W$W4)^2)/length(dw1@W$W4))
s25 <- log2(sum((dw2@W$W5)^2)/length(dw1@W$W5))
s26 <- log2(sum((dw2@W$W6)^2)/length(dw1@W$W6))
s27 <- log2(sum((dw2@W$W7)^2)/length(dw1@W$W7))
s28 <- log2(sum((dw2@W$W8)^2)/length(dw1@W$W8))
s29 <- log2(sum((dw2@W$W9)^2)/length(dw1@W$W9))
s210 <- log2(sum((dw2@W$W10)^2)/length(dw1@W$W10))
jw <- seq(from=1, to=10, by=1)
hw2 <- data.frame(jw, c(s21, s22, s23, s24, s25, s26, s27, s28, s29, s210))
names(hw2)[1] <- 'I'
names(hw2)[2] <- 'H'
data.allhw2 <- hw2
n2graph <- ggplot(data=data.allhw2, aes(x=as.numeric(data.allhw2$I),
      y=as.numeric(data.allhw2$H)) ) + theme_minimal()+labs(x="level j",
      y="H function") + geom_point(colour="olivedrab", size=1)
      + geom_smooth(method='lm', formula=y~x, colour="olivedrab",
      se=FALSE) + ylim(-10,5)
png(file = "f4_9.png", bg = "transparent", res = 600,width = 3200,
      height = 2000, units = "px")
print(n2graph)
dev.off()
lm(H ~ I, data = data.allhw2)

```

Stochastic process

```

x <- listCHFJPYr[1:1930,]
y <- listEUROJPYr[1:1930,]
mu <- c(0,0)
var(x)
var(y)
cov(x,y)
S <- matrix(c(var(x),cov(x,y),cov(x,y),var(y)), 2, 2)
df <- 4
f <- dmvtn(cbind(x,y), mu, S, df)
scatter3D(x, y, f, pch = ".", col = "#B22222", bty = "f", cex = 2, colkey = FALSE)
dev.copy(png,'f4_10.png')

```

```
dev.off()
```

Coherence function

```
H1 <- 0.8613
H2 <- 0.8789
cte <- (gamma((H1+H2+1)^2))/((gamma(2*H1+1))*gamma(2*H2+1))
k1 <- (sin((pi/2)*(H1+H2)))*(sin((pi/2)*(H1+H2)))
k2 <- (cos((pi/2)*(H1+H2)))*(cos((pi/2)*(H1+H2)))
k3 <- sin(pi*H1)
k4 <- sin(pi*H2)
k5 <- k3*k4
1/(cte/k5)
a2<-k1/(1/(cte/k5))
b2<-k2/(1/(cte/k5))
```

Simulated data

FBM1, $H = 0.89$

```
H=0.89; N=2000; T=1; L=1; M=T*N
m = rep(0, 2000)
S <- matrix(0, M, N)
for(i in 1:M) {
  for(j in 1:N) {
    S[i,j]<-((1/2)*(((i/M)^(2*H))+((j/M)^(2*H))-(abs((i/M)-(j/M))^(2*H))))
  }
}
rt <- mvrnorm(2000, mu= m, Sigma = S)
rt <- mvrnorm( mu= m, Sigma = S)
j <- seq(from=1, to=2000, by=1)
hb <- data.frame(j, rt)
names(hb)[1] <- 'Dato'
names(hb)[2] <- 'FBM'
data.allhb <- hb
phb <- ggplot(data=data.allhb, aes(x= as.numeric(data.allhb$Dato),
  y= as.numeric(data.allhb$FBM))) + theme_minimal() +
  labs(x="Data", y="FBM1") + geom_line(colour= "#CD1076")
```

```
png(file = "f4_12.png", bg = "transparent", res = 600,width = 3200,
     height = 2000, units = "px")
print(phb)
dev.off()
```

FBM1, $H = 0.87$

```
H=0.87; N=2000; T=1; L=1; M=T*N
m2 = rep(0, 2000)
S2 <- matrix(0, M, N)
for(i in 1:M) {
  for(j in 1:N) {
    S2[i,j]<-(1/2)*(((i/M)^(2*H))+((j/M)^(2*H))-(abs((i/M)-(j/M))^(2*H)))
  }
}
rt2<- mvrnorm( mu= m2, Sigma = S2)
j<-seq(from=1, to=2000, by=1)
hb2<-data.frame(j, rt2)
names(hb2)[1] <- 'Dato'
names(hb2)[2] <- 'FBM'
data.allhb2 <- hb2
phb2 <- ggplot(data=data.allhb2, aes(x= as.numeric(data.allhb2$Dato),
                                     y= as.numeric(data.allhb2$FBM))) + theme_minimal() +
  labs(x="Data", y="FBM2") + geom_line(colour= "#7D26CD")
png(file = "f4_13.png", bg = "transparent", res = 600,width = 3200,
     height = 2000, units = "px")
print(phb2)
dev.off()
```

Regression line on $FMB_1, H = 0.89$

```
dw1 <- dwt(rt, n.levels = 10, boundary="reflection", fast=FALSE)
s1 <- log2(sum((dw1@W$W1)^2)/length(dw1@W$W1))
s2 <- log2(sum((dw1@W$W2)^2)/length(dw1@W$W2))
s3 <- log2(sum((dw1@W$W3)^2)/length(dw1@W$W3))
s4 <- log2(sum((dw1@W$W4)^2)/length(dw1@W$W4))
s5 <- log2(sum((dw1@W$W5)^2)/length(dw1@W$W5))
s6 <- log2(sum((dw1@W$W6)^2)/length(dw1@W$W6))
```

```

s7 <- log2(sum((dw1@W$W7)^2)/length(dw1@W$W7))
s8 <- log2(sum((dw1@W$W8)^2)/length(dw1@W$W8))
s9 <- log2(sum((dw1@W$W9)^2)/length(dw1@W$W9))
s10 <- log2(sum((dw1@W$W10)^2)/length(dw1@W$W10))
jw <- seq(from=1, to=10, by=1)
hw <- data.frame(jw, c(s1, s2, s3, s4, s5, s6, s7, s8, s9, s10))
names(hw)[1] <- 'I1'
names(hw)[2] <- 'H1'
data.allhw <- hw
fbm1 <- ggplot(data=data.allhw, aes(x=as.numeric(data.allhw$I1),
      y=as.numeric(data.allhw$H1))) + theme_minimal()+labs(x="level j",
      y="FBM1") + geom_point(colour="#CD1076", size=1) +
      geom_smooth(method='lm', formula=y~x, colour="#CD1076",
      se=FALSE, size=0.5)
png(file = "f4_14.png", bg = "transparent", res = 600,width = 3200,
      height = 2000, units = "px")
print(fbm1)
dev.off()
lm(H1~I1, data = data.allhw)

```

Regression line on FMB_2 , $H = 0.87$

```

dw2 <- dwt(rt2, n.levels = 10, fast = FALSE)
e1 <- log2(sum((dw2@W$W1)^2)/length(dw2@W$W1))
e2 <- log2(sum((dw2@W$W2)^2)/length(dw2@W$W2))
e3 <- log2(sum((dw2@W$W3)^2)/length(dw2@W$W3))
e4 <- log2(sum((dw2@W$W4)^2)/length(dw2@W$W4))
e5 <- log2(sum((dw2@W$W5)^2)/length(dw2@W$W5))
e6 <- log2(sum((dw2@W$W6)^2)/length(dw2@W$W6))
e7 <- log2(sum((dw2@W$W7)^2)/length(dw2@W$W7))
e8 <- log2(sum((dw2@W$W8)^2)/length(dw2@W$W8))
e9 <- log2(sum((dw2@W$W9)^2)/length(dw2@W$W9))
e10 <- log2(sum((dw2@W$W10)^2)/length(dw2@W$W10))
je <- seq(from=1, to=10, by=1)
he <- data.frame(je, c(e1, e2, e3, e4, e5, e6, e7, e8, e9, e10))
names(he)[1] <- 'I2'
names(he)[2] <- 'H2'

```

```

data.allhe <- he
fbm2 <- ggplot(data=data.allhe, aes(x=as.numeric(data.allhe$I2),
  y=as.numeric(data.allhe$H2)) ) + theme_minimal() + labs(x="level j ",
  y="FBM2") + geom_point(colour="#7D26CD", size=1) +
  geom_smooth(method='lm', formula=y ~ x, colour="#7D26CD",
  se=FALSE, size=0.5)
png(file = "f4_15.png", bg = "transparent", res = 600,width = 3200,
  height = 2000, units = "px")
print(fbm2)
dev.off()
lm(H2~I2, data = data.allhe)

```

Coherence function

```

H1 <- 0.89
H2 <- 0.87
cte <- (gamma((H1+H2+1)^2))/((gamma(2*H1+1))*gamma(2*H2+1))
k1 <- (sin((pi/2)*(H1+H2)))*(sin((pi/2)*(H1+H2)))
k2 <- (cos((pi/2)*(H1+H2)))*(cos((pi/2)*(H1+H2)))
k3 <- sin(pi*H1)
k4 <- sin(pi*H2)
k5 <- k3*k4
1/(cte/k5)
a2<-k1/(1/(cte/k5))
b2<-k2/(1/(cte/k5))

```